

CAUSAL CLASSIFICATION OF PATHOLOGICAL MISNER-TYPE SPACETIMES

N. E. RIEGER

MATHEMATICS DEPARTMENT, UNIVERSITY OF CALIFORNIA IRVINE, ROWLAND HALL, 92697 IRVINE, USA
CURRENT ADDRESS: MATHEMATICS DEPARTMENT, YALE UNIVERSITY, 219 PROSPECT STREET, NEW
HAVEN, CT 06520, USA
N.RIEGER@YALE.EDU

ABSTRACT. We investigate three causality-violating spacetimes: Misner space (including Kip Thorne’s “moving wall” model), the pseudo-Schwarzschild spacetime, and a new model introduced here, the pseudo-Reissner-Nordström spacetime. Despite their different physical origins—ranging from a flat vacuum solution to a black-hole-type vacuum solution to a non-vacuum model requiring exotic matter—all three share a common warped-product structure, 2-dimensional cylindrical base metrics of Eddington-Finkelstein type, and fundamental causal features such as Cauchy and chronology horizons, acausal regions, and analogous geodesic behaviour. Building on a conjecture first proposed in 2016, we present a formal proof that the three models are *pairwise isocausal* on their universal covers and on suitable causally regular regions of their compactified forms. The proof is constructive, providing explicit causal bijections between the models and identifying a concrete deck-equivariance criterion for when the isocausality descends to the compactified spacetimes. In the absence of equivariance, the covering result does not imply global isocausality, and at most a one-way causal relation holds between the compactified models. These results supply a rigorous causal classification linking these spacetimes, placing them within a unified Misner-type family and providing a framework for extending the classification to other causality-violating solutions.

This article is based on research originally conducted as part of a project during 2016-2018 under the supervision of Kip S. Thorne.

1. INTRODUCTION

General relativity defines a class of cosmological models, each representing an idealization of a physically possible universe compatible with the theory. A cosmological model is a mathematical description of this idealized universe, referred to as a spacetime and represented by a pair (M, g) , where M is a differentiable manifold capturing the topology and continuity of the universe, and g is a smooth, symmetric, non-degenerate $(0, 2)$ -tensor field encoding the geometric and causal structure. Each point in M represents an event, and the causal structure determined by g governs the possible trajectories of particles and light rays. Within this framework, the theoretical possibility of time travel—through closed timelike curves (CTCs) that allow a timelike observer to return to an event in their own past—has been studied extensively [1, 4, 9, 19, 12, 21, 22]. In 1967, Charles Misner introduced the Misner space [14] as a minimal example of a spacetime with a chronology-violating region. While constructing spacetimes containing CTCs is relatively straightforward, finding examples with a plausible physical interpretation is more challenging. The pseudo-Schwarzschild spacetime, proposed by Ori [16] in 2007, is a more sophisticated causality-violating model that incorporates

features such as Cauchy horizons, avoids singularities, and models the breakdown of determinism inside black holes.¹

We begin by examining these two apparently different spacetimes—Misner space (also in the form of Kip Thorne’s “moving wall” model) and the pseudo-Schwarzschild spacetime—to clarify their geometric structures and causal properties, with a particular focus on pathologies. The two are linked by their chronological and global features. Indeed, the pseudo-Schwarzschild spacetime can be viewed as a non-flat generalization of Misner space: in the limit as the mass parameter $M \rightarrow 0$, the pseudo-Schwarzschild metric reduces to the Misner metric. In earlier work [18] we conjectured that these spacetimes are *isocausal* in the sense of García-Parrado and Senovilla.

We then introduce a new chronology-violating spacetime: the *pseudo-Reissner-Nordström* spacetime, which generalizes the previous two by including an electric charge parameter in analogy with the classical Reissner-Nordström solution. Like its predecessors, this model possesses Cauchy and chronology horizons, acausal regions, and a warped-product structure with a 2-dimensional cylindrical base and hyperbolic spatial fibers. Its inclusion is especially noteworthy because it is a non-vacuum solution, in contrast to the vacuum nature of Misner and pseudo-Schwarzschild spacetimes, yet it still exhibits the same characteristic causal pathologies.

A central contribution of this paper is to *replace the earlier conjecture with a formal proof* that all three spacetimes—Misner, pseudo-Schwarzschild, and pseudo-Reissner-Nordström—are *pairwise isocausal* on their universal covers, and on suitable open, causally regular regions of the compactified spacetimes. Proposition 7.1 provides explicit causal bijections between the models in Eddington-Finkelstein-type coordinates, and identifies a concrete *deck-equivariance criterion* under which this isocausality descends to the compactified spacetimes themselves. Corollary 1 and Remark 7.2 clarify that, in the generic case where this criterion fails, one obtains only a *one-way causal relation* globally, despite the mutual isocausality of the covering spaces. This sharpens the classification of these causality-violating models and establishes, for the first time, a rigorous causal equivalence framework connecting them.

From a mathematical perspective, the shared warped-product structure and conformal relation of the base metrics make these isocausality results natural; from a physical perspective, the fact that such structurally and interpretatively different spacetimes exhibit identical causal behaviour is striking. This work provides a unified geometric and causal framework for understanding these examples, and paves the way for extending the classification to other models—such as the pseudo-Kerr spacetime—that may also belong to this Misner-type, causality-violating family.

1.1. Causality violating spacetimes. Before presenting the main results we want to review some useful definitions.

First, recall that a Lorentzian manifold M is said to be *past-distinguishing* if any two points $p, q \in M$ with identical chronological pasts must coincide; that is, $I^-(p) = I^-(q) \implies p = q$. Similarly, M is said to be *future-distinguishing* if any two points $p, q \in M$ the same chronological future must be identical: $I^+(p) = I^+(q) \implies p = q$. We say a spacetime satisfies the *distinguishability condition* if it is both, past- and future-distinguishing. Thus, a Lorentzian manifold is *not* past-distinguishing if distinct points can have identical pasts. A spacetime allows time travel if a point $p \in M$ lies in its own timelike future, i.e., $p \in I^+(p)$, resulting in a closed timelike curve that violates causality. Hence, for distinct points $p, q \in M$,

¹An “idealized black hole model” is a simplified theoretical depiction of a black hole, commonly assuming perfect spherical symmetry and no rotation, and typically derived from the Schwarzschild metric.

it is possible to have $p \ll q \ll p$. The *chronology violating region* of a spacetime (M, g) is defined as $\mathcal{V}(M) = \{p \in M : p \in I^+(p)\}$.²

Definition 1.1. A spacetime (M, g) is said to be *chronological* and to satisfy the *chronology condition* if it does not contain any closed timelike curves; that is, $p \notin I^+(p)$ for all $p \in M$.

Proposition 1.2. [10] *If the spacetime (M, g) is compact then the chronology violating region is not empty and contains a closed timelike curve.*

Definition 1.3. A subset $S \subset M$ is said to be *achronal* if no timelike curve intersects it more than once; that is, there do not exist points $p, q \in S$ such that $q \in I^+(p)$. Equivalently, $I^+(S) \cap S = \emptyset$.

The boundaries separating choral and achronal regions are called *chronology horizons*. The choral region ends and closed timelike curves arise at the future chronology horizon. Conversely, closed timelike curves vanish and the choral region begins at the past chronology horizon. A future chronology horizon is a special type of future Cauchy horizon and it is therefore subject to all the properties of such horizons [5]. The *past chronology horizon* is defined dually.

Definition 1.4. Let $J^-(U)$ denote the causal past of a set $U \subset M$, and let $\bar{J}^-(U)$ represent the topological closure of J^- . Define \mathcal{I}^+ and \mathcal{I}^- as future and past null infinity, respectively. The *boundary* of \bar{J}^- is given by $\partial\bar{J}^-(U) = \bar{J}^-(U) \setminus J^-(U)$, and the *future event horizon* of M is $\mathcal{H}^+ = \partial\bar{J}^-(\mathcal{I}^+)$.

The event horizon is often referred to as the ‘‘point of no return’’. It is useful to define $\bar{J}^-(\mathcal{I}^+)$ as the *domain of outer communications*. The complement $M \setminus \bar{J}^-(\mathcal{I}^+)$ is then referred to as the *black hole* (region). A spacetime may contain a singularity in several senses. In this context, a singularity is a hypersurface on which all worldlines that pass through the event horizon terminate.

2. MISNER SPACE

Misner space [14], typically presented as a 2-dimensional toy model, is a type of spacetime in general relativity that illustrates how singularities might form. This spacetime begins with causally well-behaved initial conditions but later develops closed timelike curves, leading to a chronology-violating region. Characterized by a conformally flat metric, Misner space is also Ricci-flat, making it a valid vacuum solution to Einstein’s field equations in the absence of matter and energy. The 4-dimensional version can be obtained as a straightforward extension. It can be considered as Minkowski space with an altered topology due to identification under a boost.³ To see this, start with the Lorentz-Minkowski spacetime $\mathcal{M} := (\mathbb{R}^4, \tilde{\eta})$, defined as the smooth manifold $\mathbb{R}^{1,3} := (\mathbb{R}^4, \tilde{\eta})$ equipped with Lorentzian coordinates $(\tilde{t}, \tilde{x}_1, \tilde{x}_2, \tilde{x}_3)$. These coordinates yield the metric tensor $\tilde{\eta}$, given by

$$(2.1) \quad ds^2 := -d\tilde{t}^2 + (d\tilde{x}_1)^2 + (d\tilde{x}_2)^2 + (d\tilde{x}_3)^2.$$

This coordinate system for Minkowski spacetime is related to Misner coordinates (η, X_1, X_2, X_3) through the following coordinate transformation

²The set $\mathcal{V}(M)$ decomposes into equivalence classes $[p]$, where $p \sim q$ if $p \ll q \ll p$. That is, two points $p, q \in [p]$ belong to the same equivalence class if there exists a closed timelike curve γ connecting p and q with $\gamma(I) \subset [p]$. Points within the same equivalence class share the same chronological character, making it impossible to establish a definite chronological order of events among them.

³A Lorentz boost is a Lorentz transformation with no rotation.

$$(2.2) \quad \tilde{t} = 2\sqrt{\eta} \cosh\left(\frac{X_1}{2}\right), \quad \tilde{x}_1 = 2\sqrt{\eta} \sinh\left(\frac{X_1}{2}\right), \quad \tilde{x}_2 = X_2, \quad \tilde{x}_3 = X_3.$$

This coordinate change results in the Misner metric $ds^2 = -\eta^{-1}d\eta^2 + \eta(dX_1)^2 + (dX_2)^2 + (dX_3)^2$, where $0 < \eta < \infty$, $0 \leq X_1 \leq 2\pi$ as an angular coordinate, and $-\infty \leq X_2, X_3 \leq \infty$. Due to the periodic nature of the coordinate X_1 , the underlying topology is given by $S^1 \times \mathbb{R}^3$. However, at $\eta = 0$ the metric exhibits an apparent (coordinate) singularity. To address this, we introduce a new set of coordinates to extend the metric beyond $\eta = 0$. Specifically, we define a new coordinate $\varphi = X_1 - \ln(\eta)$. To transform the metric accordingly, we also require $d\varphi = dX_1 + \frac{d\eta}{\eta}$. Thus, the metric transforms into $ds^2 = 2d\eta d\varphi + \eta d\varphi^2 + (dX_2)^2 + (dX_3)^2$. Finally, since η is a timelike coordinate, we introduce the substitution $T = \eta$, leading to the metric

$$(2.3) \quad ds^2 = 2dTd\varphi + Td\varphi^2 + (dX_2)^2 + (dX_3)^2,$$

where T is a timelike coordinate and φ is an angular coordinate, with domains $-\infty < T < \infty$ and $0 \leq \varphi \leq a$.⁴ Note that this is only one of two possible inequivalent extensions of Misner space. Alternatively, we could start with the Minkowski metric (2.1) again, but apply a different coordinate transformation, subsequently extending the resulting Misner space across the coordinate singularity in a different way. In both cases, we obtain a cylindrical Misner spacetime defined on $M = S^1 \times \mathbb{R}^3$.

Accordingly, Minkowski space \mathcal{M} serves as the associated covering space of Misner space, where identical points are determined by the identification

$$(2.4) \quad (\tilde{t}, \tilde{x}_1, \tilde{x}_2, \tilde{x}_3) \leftrightarrow (\tilde{t} \cosh(na) + \tilde{x}_1 \sinh(na), \tilde{t} \sinh(na) + \tilde{x}_1 \cosh(na), \tilde{x}_2, \tilde{x}_3),$$

where a is the period associated with the periodic direction X_1 .⁵

We orient Misner space in time by requiring $-\partial_T$ to point toward the future. The vector field ∂_T is everywhere lightlike, while ∂_φ is spacelike for $T > 0$, lightlike at $T = 0$, and timelike for $T < 0$. At $T = 0$, there exists a null surface known as the *chronology horizon*, which separates the chronology-violating region from the choral region. This surface is intersected exactly once by every causal curve, thereby serving as the Cauchy horizon for any initial hypersurface with $T_0 = \text{const} > 0$. Hypersurfaces of constant $T = \text{const} > 0$ are spacelike and can be chosen as initial data hypersurfaces for specifying the evolution of fields.

Proposition 2.1. *If a closed timelike curve (CTC) arises in a chronology-violating spacetime, then it contains an unlimited number of CTCs.*

Proof. Let α be a closed timelike curve in the spacetime M . Then consider two points p and q on α that satisfy the condition $p \ll q$. Consequently, we have $p \ll q \ll p$ and $p \in I^+(p)$ as well as $q \in I^+(q)$. The same applies for the timelike past. The sets $I^+(p)$ and $I^-(q)$ are open and their finite intersection $O := I^+(p) \cap I^-(q)$ is therefore not empty and an open set as well. Choose now any $r \in O$. Since $r \in I^+(p)$ there is a future directed timelike curve segment from p to r , and because $r \in I^-(q)$, there is a future directed timelike curve segment from q to r . It remains to join the two curve segments at the point r which can be done smoothly due to the fact that O is an open neighborhood of r . \square

⁴Due to the periodicity condition, φ can take any real number value. Specifically, φ and $\varphi + na$ are equivalent for any integer n .

⁵Note, that these points correspond to $(\eta, X_1, X_2, X_3) \leftrightarrow (\eta, X_1 + na, X_2, X_3)$ in Misner coordinates.

tilt or open. Due to the special relativistic time dilation, a region with closed timelike curves develops, see Figure 1.

Note that the worldline of the clock at rest (along the t -axis) and the worldline of the clock in motion (along the \bar{t} -axis) are identified by \sim , meaning the events along these lines are physically identical. However, due to special relativity, the observer at rest perceives the moving clock to tick more slowly. On the t -axis we have $\tau = t$, while on the \bar{t} -axis, due to time dilation, $\tau = \frac{t}{\sqrt{1-\beta^2}} = \gamma t$, where $\gamma := \frac{1}{\sqrt{1-\frac{\beta^2}{c^2}}} = \frac{1}{\sqrt{1-\beta^2}}$.

Connection to mathematical approach. In the style of [12], we set the proper time origins, $\tau = 0$, such that they are separated by the chronology horizon at $x = t$. We denote the spatial distance between these $\tau = 0$ origins as D .

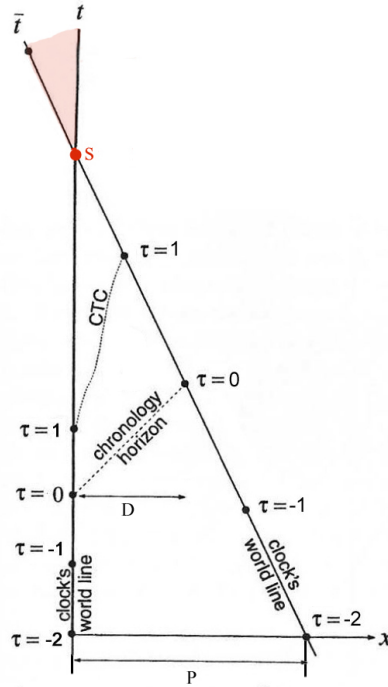


FIGURE 2. ‘Moving wall’ Misner space with proper time origins, such that the two walls are separated by the chronology horizon at $x = t$ by the spatial distance D .

The left wall ($t = \tau$, $x = 0$) in this example is at rest in Lorentzian coordinates, while the right wall ($x = D - \beta\gamma\tau$, $t = D + \gamma\tau$) moves towards the left one with constant velocity β . The location of the chronology horizon depends on D , which can be any positive constant, and the speed β with $|\beta| < 1$. All further boosted copies of Misner space depend on this initial choice of D and β . Provided $\beta \neq 0$, the two walls intersect at a point s , see Figure 2. This point, as well as the region beyond it, raises questions about their nature. We can better address these questions with the aid of the covering space, as depicted in Figure 3.

Calculation of intersection points. We can describe the ‘moving wall’ model of Misner space by switching to the covering space [22]. Side by side, we line up copies of Misner space that are identified through the action of a boost with speed β . In comparison to Figure 2, W_0 corresponds to t , and W_1 corresponds to \bar{t} . Additionally, the boost induces an equivalence relation, identifying boost-related points p under \sim , all of which lie on hyperbolas defined by $\tilde{t}^2 - \tilde{x}^2 = \text{const}$.

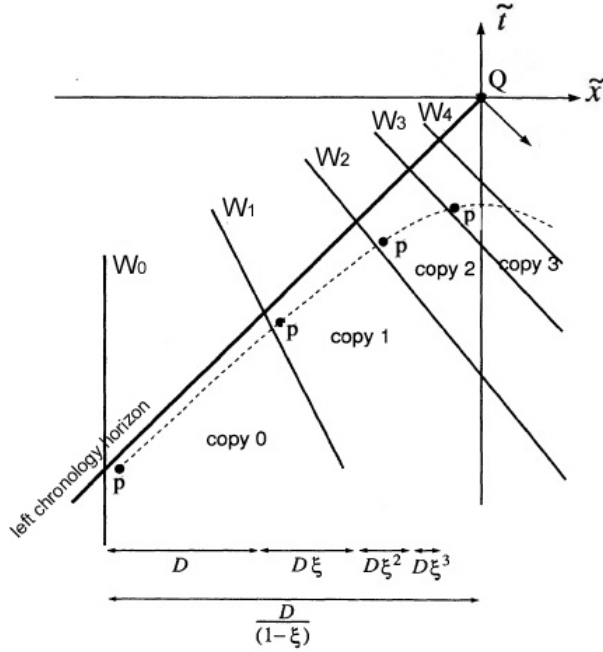


FIGURE 3. Covering space for the ‘moving wall’ model of Misner space. The singularity manifests as the intersection point Q of the left and right chronology horizons.

The relation between the covering space in Minkowski coordinates (\tilde{t}, \tilde{x}) and the Minkowski coordinates (t, x) in the ‘moving wall’ model of Misner space (*copy 0*) is given by [12]

$$(2.5) \quad \tilde{t} = t - \frac{D}{1-\xi}$$

and

$$(2.6) \quad \tilde{x} = x - \frac{D}{1-\xi},$$

where $\xi = \sqrt{\left(\frac{1-\beta}{1+\beta}\right)}$ is the Doppler blueshift. In the covering space (Figure 3) we get the spatial distance between W_0 and the \tilde{t} -axis by the converging series

$$D\xi^0 + D\xi^1 + D\xi^2 + D\xi^3 \dots = D \cdot \sum \xi^i = D \cdot \frac{1}{1-\xi},$$

for $|\xi| < 1$. Thus, the left wall of *copy* 0, denoted W_0 , is located at $\tilde{x} = \frac{-D}{1-\xi}$, and the right wall, W_1 , of *copy* 0 is located at

$$\left(\tilde{t} + \frac{\xi D}{1-\xi}\right) = \left(\frac{1+\xi^{-2}}{1-\xi^{-2}}\right)\left(\tilde{x} + \frac{\xi D}{1-\xi}\right).$$

Hence,

$$(2.7) \quad \left(\frac{1+\xi^{-2(n+1)}}{1-\xi^{-2(n+1)}}\right)\left(\tilde{x} + \frac{\xi^{n+1}D}{1-\xi}\right) - \frac{\xi^{n+1}D}{1-\xi} = \left(\frac{1+\xi^{-2n}}{1-\xi^{-2n}}\right)\left(\tilde{x} + \frac{\xi^n D}{1-\xi}\right) - \frac{\xi^n D}{1-\xi}$$

yields the intersection of two adjacent walls, $W_n \cap W_{n+1} = s_n = (\tilde{t}_n, \tilde{x}_n)$:

$$(2.8) \quad \tilde{t}_n = \frac{D\xi^{-n}(\xi^{1+2n} - 1)}{\xi^2 - 1}$$

$$(2.9) \quad \tilde{x}_n = \frac{D\xi^{-n}(\xi^{2n+1} + 1)}{\xi^2 - 1}.$$

Each point s_n is on the hyperboloid

$$(2.10) \quad \tilde{t}_n^2 - \tilde{x}_n^2 = -\frac{4\xi D^2}{(\xi^2 - 1)^2} = \text{const.}$$

Clearly, we have $\tilde{t}_{n+1}^2 - \tilde{x}_{n+1}^2 = \tilde{t}_n^2 - \tilde{x}_n^2$ so the points s_{n+1} and s_n lie on the same hyperboloid. From this, we can conclude that each point s_n is taken by a boost to s_{n+1} . Thus, the points s_n belong to the same fiber over a specific point in the Misner base space and can be regarded as physically identical, as they are mapped by the covering map onto identical events in Misner space.

We turn again to the covering space (see Figure 4), we focus on the intersection points and the regions beyond them. At first glance, the seemingly inconsistent distribution of intersection points s_n might appear to contradict the definition of the covering space, which is constructed as a union of disjoint sets (in our case, a disjoint union of copies of Misner space). However, this non-chronological structure simply reflects the chronology-violating nature of region *III*, as explained in [11].

by two chronology horizons. Like the future chronology horizon \mathcal{H}_+ , the past chronology horizon \mathcal{H}_- is a null surface.

Given that the initial choice of the wall W_0 and the speed β are arbitrary, we can obtain the covering space without coordinate singularities [17] by appropriately selecting these initial conditions (as shown in Figure 5). The covering space corresponds to the left half-plane of Minkowski space.

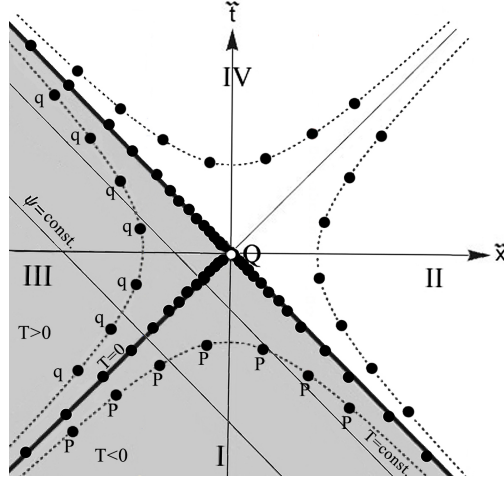


FIGURE 5. Universal covering space for Misner space with the metric $ds^2 = Td\psi^2 + 2dTd\psi$. The transformation between the covering space coordinates and Misner coordinates is given by $\psi = -2\ln(\frac{\tilde{t}-\tilde{x}}{2})$, $T = \frac{\tilde{t}^2-\tilde{x}^2}{4}$.

2.2. Geodesics for warped Misner product space. The 4-dimensional Misner space (2.3) can be expressed as a warped product space of the form $M = M_Z \times_r H^2$, where M_Z is the 2-dimensional Misner-type spacetime with coordinates (T, φ) , and H^2 is the 2-dimensional hyperbolic plane, described by coordinates (θ, ϕ) . The general form of the metric combines the 2-dimensional Misner-type geometry, which encodes the non-trivial topological and causal structure, with a 2-hyperbolic plane that introduces hyperbolic symmetry. The metric can be written as

$$ds^2 = f(T)(d\varphi)^2 + 2dTd\varphi + r^2(d\theta^2 + \sinh^2 \theta d\phi^2),$$

where $f(T)$ describes the time-dependent geometry of the Misner-type spacetime and r is the warping function. To interpret this, we consider \mathbb{R}^2 as being represented topologically by the hyperbolic plane H^2 . The 4-dimensional Misner space can then be described as a warped product $M := M_Z \times_r H^2$, with the warping function r being a scalar function $r : M_Z \rightarrow \mathbb{R}$, depending on the coordinates of the base manifold M_Z . The Misner space $M_Z = S^1 \times \mathbb{R}$ is equipped with the cylindrical metric $ds^2 = 2dTd\varphi + Td\varphi^2$. The fiber H^2 , with coordinates (θ, ϕ) , has the hyperbolic metric $g_{H^2} = d\theta^2 + \sinh^2 \theta d\phi^2$, scaled by r^2 . Therefore, the metric on the total space M can be written as $ds^2 = g_Z + r^2 g_{H^2}$, which explicitly expands to

$$ds^2 = 2dTd\varphi + Td\varphi^2 + r^2(d\theta^2 + \sinh^2 \theta d\phi^2),$$

where the warping function r is given by $r = T \exp(\frac{\varphi}{2}) - \exp(-\frac{\varphi}{2})$. If r is constant, the warped product reduces to a direct product of the base M_Z and fiber H^2 .

Remark 2.2. The surface H_r^2 , also known as a pseudo-sphere, has constant negative Gaussian curvature of -1 , which provides the desired high symmetry. The upper sheet of the pseudo-sphere is given by the set

$$H_r^2 = \{(z, x, y) \in \mathbb{R}_1^3 : -z^2 + x^2 + y^2 = -r^2, z > 0\}.$$

Based on the warped geometry of Misner space, we can focus on the embedded cylinders defined by $\theta = \text{const}$ and $\varphi = \text{const}$. By doing so, we restrict our attention to the 2-dimensional Misner cylinder M_Z , which captures the essential features of the Misner-type geometry.

Here, we examine the geodesic equations, which show that there exist incomplete null and timelike geodesics that spiral around the cylinder and cannot be extended. One class of these incomplete timelike geodesics not only orbits around the chronology horizon but also penetrates the null surface into negative T , where it reaches a turning point, intersects itself, and then encircles the cylinder below the horizon.

Given the 2-dimensional Misner metric $ds^2 = Td\varphi^2 + 2dTd\varphi$, null geodesics are described by

$$(2.11) \quad \begin{cases} \psi(T) = \text{const.} & (\text{outgoing}) \\ \psi(T) = \int -\frac{2}{T}dT & (\text{ingoing}) \end{cases},$$

where outgoing null geodesics are complete, while ingoing ones circle around the Misner cylinder infinitely often near the Cauchy horizon. For timelike geodesics, we use the expression

$$(2.12) \quad \psi(T) = \int \frac{\dot{\psi}}{\dot{T}} dT.$$

Substituting $\dot{\psi}$ and \dot{T} , we get:

$$\psi(T) = \frac{\frac{1}{T}(\xi - \omega\sqrt{\xi^2 + T})}{\omega\sqrt{\xi^2 + T}} dT = \int \frac{1}{T} \left(\frac{\omega}{\sqrt{1 + \frac{T}{\xi^2}}} - 1 \right) dT,$$

with $\xi \equiv \text{const}$ and $\omega = \pm 1$ for outgoing and ingoing geodesics, respectively. There are two families of timelike geodesics and both of them are incomplete. One class of geodesics does not cross the Cauchy horizon and spirals around the cylinder just above $T = 0$. A geodesic from the other class, however, crosses the Cauchy horizon, entering the chronology-violating region. It reaches a turning point at $T = -\xi^2$, where the particle's velocity vanishes, as shown by the condition

$$\omega\sqrt{\xi^2 + T} = 0 \Leftrightarrow \sqrt{\xi^2 + T} = 0 \Leftrightarrow T = -\xi^2.$$

Therefore, a massive particle cannot reach $T = -\infty$. Such a timelike geodesic intersects itself as it tracks back, converging towards the Cauchy horizon and spiraling around the Misner cylinder just below $T = 0$. In contrast, there is no such behavior for photons, and there is no obstruction for null geodesics to reach $T = -\infty$.

This result implies that geodesics encircle the extended Misner cylinder with increasingly higher frequencies as they approach $T = 0$, asymptotically nearing the chronology horizon. The singular point Q represents

a genuine spacetime pathology: geodesic incompleteness in this case could correspond to a rocket ship suddenly disappearing from the universe after a finite amount of proper time. As shown in Subsection 2.1, this pathological nature of the geodesics becomes evident in the covering space, where the geodesic singularity manifests as the intersection point Q of the left and right chronology horizons [22], as illustrated in Figure 4.

3. GENERAL EQUATIONS FOR RADIAL GEODESICS

In this section, we present a complete canonical formulation of the geodesic equations for cylindrical Misner-type spacetime models, focusing on the embedded $\theta = \text{const}$ and $\varphi = \text{const}$ cylinders, as introduced in Subsection 2.2. We anticipate that the radial geodesic equations for the pseudo-Schwarzschild and pseudo-Reissner-Nordström spacetimes (to be discussed in Sections 4 and 6) will exhibit structural similarities. To unify these cases, we derive a general form of the geodesic equations, which proves to be valid for all three hyperbolically symmetric spacetimes. Notably, this general form can also be applied to Misner space, recognizing that the 2-dimensional Misner metric, $ds^2 = Td\varphi^2 + 2dTd\varphi$, can be rewritten in the canonical form

$$(3.1) \quad ds^2 = f(r)d\nu^2 + 2d\nu dr,$$

where $f(r) = g_{\nu\nu}$. This metric, due to its geodesic singularity at Q , is commonly referred to as the canonical quasi-singular metric [13].

To generalize the Equation 3.1 to the 4-dimensional case for hyperbolically symmetric models, we start with the general form of a hyperbolically symmetric metric given by

$$(3.2) \quad ds^2 = g_{\nu\nu}d\nu^2 + 2g_{\nu r}d\nu dr + r^2(d\theta^2 + \sinh^2\theta d\phi^2).$$

Since we are strictly interested in geodesics for radial motion, we can safely set $\phi = 0$ and $\theta = \frac{\pi}{2}$. Furthermore, we impose the metric condition resulting from the causal character of the geodesics

$$(3.3) \quad g_{\nu\nu}\dot{\nu}^2 + 2g_{\nu r}\dot{\nu}\dot{r} \equiv k,$$

where $k = -1$ for timelike, $k = +1$ for spacelike, and $k = 0$ for null geodesics. The time coordinate ν is cyclic, and we always have $g_{\nu r} = 1$, so we obtain the constant term

$$\frac{\partial(\frac{1}{2}g_{\nu\nu}\dot{\nu}^2 + \dot{r}\dot{\nu})}{\partial\dot{\nu}} = g_{\nu\nu}\dot{\nu} + \dot{r} \equiv \xi.$$

This is equivalent to $\dot{\nu} = g^{\nu\nu}(\xi - \dot{r})$, and substituting this into Equation (3.3) gives

$$g_{\nu\nu}[g^{\nu\nu}(\xi - \dot{r})]^2 + 2\dot{r}[g^{\nu\nu}(\xi - \dot{r})] = k \iff \dot{r}^2 = \xi^2 - kg_{\nu\nu}.$$

For a circular orbit, the geodesic equation [20] is also given by $\ddot{r} = -\frac{mk}{r^2}$.

Assembling these results, we obtain the equations

$$(3.4) \quad \dot{\nu} = g^{\nu\nu} \left(\xi - \omega \sqrt{\xi^2 - kg_{\nu\nu}} \right)$$

$$(3.5) \quad \dot{r} = \omega \sqrt{\xi^2 - kg_{\nu\nu}},$$

where ω has been chosen to represent outgoing geodesics for $\omega = +1$, and ingoing geodesics for $\omega = -1$. Now, the function of r that is suitable for our study of geodesics can be inferred:

$$(3.6) \quad \nu(r) = \int \frac{\dot{\nu}}{\dot{r}} dr = \int \frac{g^{\nu\nu} (\xi - \omega \sqrt{\xi^2 - kg_{\nu\nu}})}{\omega \sqrt{\xi^2 - kg_{\nu\nu}}} dr = \int \frac{1}{g_{\nu\nu}} \left(\frac{\omega}{\sqrt{1 - \frac{kg_{\nu\nu}}{\xi^2}}} - 1 \right) dr.$$

In the case of timelike geodesics this gives

$$(3.7) \quad \nu(r) = \int \frac{g^{\nu\nu} (\xi - \omega \sqrt{\xi^2 + g_{\nu\nu}})}{\omega \sqrt{\xi^2 + g_{\nu\nu}}} dr = \int \frac{1}{g_{\nu\nu}} \left(\frac{\omega}{\sqrt{1 + \frac{g_{\nu\nu}}{\xi^2}}} - 1 \right) dr,$$

and for null geodesics we have

$$(3.8) \quad \nu(r) = \int \frac{1}{g_{\nu\nu}} (\omega - 1) dr.$$

For timelike geodesics, the condition $\omega \sqrt{\xi^2 + g_{\nu\nu}} = 0 \iff \xi^2 + g_{\nu\nu} = 0$, with the value $-\xi^2 = g_{\nu\nu}$, corresponds to the particle either having a turning point or asymptotically approaching a horizon.

These results provide further insights. By renaming the coordinates as $\nu = \psi$ and $r = T$, we can carry over the findings to the Misner case, which takes the same general form as the 2-dimensional cylindrical pseudo-Schwarzschild (4.4) and pseudo-Reissner-Nordström (6.3) spacetimes in Eddington-Finkelstein coordinates:

$$(3.9) \quad ds^2 = f(t)dx^2 + 2dxdt.$$

4. PSEUDO-SCHWARZSCHILD SPACETIME

Although the pseudo-Schwarzschild spacetime is derived from the well-known Schwarzschild spacetime, its global and causal structure more closely resembles that of Misner space. The pseudo-Schwarzschild solution satisfies the Einstein field equations in vacuum and describes a static, hyperbolically symmetric vacuum spacetime [16]. Furthermore, its universal covering space asymptotically approaches Minkowski space, which is known as asymptotic flatness. This serves as another example of a spacetime that violates the chronology condition and allows for the existence of closed timelike curves. The geometry of the pseudo-Schwarzschild spacetime admits a warped product structure, with the base manifold $S^1 \times \mathbb{R}^+$ and the hyperbolic plane H^2 as the fiber. The point set that defines the pseudo-Schwarzschild manifold is

$$(4.1) \quad M = S^1 \times \mathbb{R}^+ \times H_r^2,$$

where S^1 is the 1-sphere, topologically equivalent to an interval whose endpoints are glued together by identification, and H_r^2 (when $t, r = \text{const}$) represents a 2-dimensional surface that can be identified with

one of the sheets of the two-sheeted space-like hyperboloid.⁷ Then the pseudo-Schwarzschild metric can be derived by performing a Wick rotation $\theta \rightarrow i\theta$ and a signature change from the famous Schwarzschild metric as follows:

$$\begin{aligned}
ds^2 &= -(1 - \frac{2m}{r})dt \otimes dt + (1 - \frac{2m}{r})^{-1}dr \otimes dr + r^2(d\theta \otimes d\theta + \sin^2(\theta)d\phi \otimes d\phi) \\
&\xrightarrow{\theta \rightarrow i\theta} ds^2 = -(1 - \frac{2m}{r})dt^2 + (1 - \frac{2m}{r})^{-1}dr^2 + r^2(d(i\theta)^2 + \underbrace{\sin^2(i\theta)}_{-\sinh^2(\theta)}d\phi^2) \\
&\xrightarrow{(-1)} ds^2 = (1 - \frac{2m}{r})dt^2 - (1 - \frac{2m}{r})^{-1}dr^2 + r^2(d\theta^2 + \sinh^2(\theta)d\phi^2).
\end{aligned}$$

We rewrite the last equation as

$$(4.2) \quad ds^2 = -(\frac{2m}{r} - 1)dt^2 + (\frac{2m}{r} - 1)^{-1}dr^2 + r^2(d\theta^2 + \sinh^2(\theta)d\phi^2),$$

where θ takes all positive values, $0 \leq \phi < 2\pi$, and $m \geq 0$, thereby obtaining the pseudo-Schwarzschild metric. However, in contrast to the Schwarzschild solution, this spacetime exhibits hyperbolic symmetry, and the coordinate t is assumed to be periodic, with $0 \leq t < a$, where the identification $(t, r, \theta, \phi) \sim (t + na, r, \theta, \phi)$ for $n \in \mathbb{N}$ is applied. Note that, due to the identification of edge-to-edge points as defined above, there is a change in the topology of the spacetime.

The periodicity of the coordinate t , after the Wick rotation, arises from the fact that the structure of the corresponding isometry group changes from the non-compact additive group \mathbb{R} to the compact group $U(1)$, which has inherently periodic orbits. In general, the real Lie algebra of the isometry group is generated by the associated Killing vector fields; that is, the infinitesimal generators of one-parameter isometry groups. However, Wick rotating a coordinate (i.e., multiplying it by i) changes the associated real Lie algebra into a different real form of a common complexified Lie algebra.

For example, the real Lie algebras of \mathbb{R} and $U(1)$ both complexify to the complex Lie algebra \mathbb{C} , which is the Lie algebra of the complex multiplicative group $\mathbb{C}^* \setminus \{0\}$. Thus, the transition between \mathbb{R} and $U(1)$ reflects a change in real form within the same complexified structure.

In the specific construction used above, this transformation arises via a *double Wick rotation*:

$$\theta \mapsto i\theta, \quad t \mapsto it.$$

Under this transformation, the isometry group associated with θ changes from $U(1)$ to \mathbb{R} , while the group associated with t changes conversely from \mathbb{R} to $U(1)$. Consequently, the new imaginary time coordinate becomes periodic due to the compactness of $U(1)$.

⁷The upper sheet of the hyperboloid can be globally embedded in 3-dimensional Minkowski space. We can express the upper sheet hyperboloid using a parameterization in polar coordinates (θ, ϕ) . Specifically, the map $\mathbb{R}^+ \times S^1 \rightarrow H_r^2$, $(\theta, \phi) \mapsto (r \cosh(\theta), r \sinh(\theta) \cos(\phi), r \sinh(\theta) \sin(\phi))$ describes the embedding of the upper sheet of the hyperboloid in Minkowski space. The hyperboloid together with the induced Riemannian metric $g = d\theta \otimes d\theta + \sinh^2(\theta)d\phi \otimes d\phi$ is called *hyperbolic plane*.

This periodicity is not merely a formal artifact but carries physical meaning. For instance, imaginary time is also periodic in the Euclidean Schwarzschild solution, where the length of the period corresponds to the inverse of the Hawking temperature of the original black hole. Hence, the periodic nature of imaginary time in the pseudo-Schwarzschild context is consistent with both geometric reasoning and physical interpretation.

Since the geometry of the pseudo-Schwarzschild spacetime can be expressed as a warped product, with the cylindrical base $M_Z := S^1 \times \mathbb{R}^+$ and the hyperbolic plane H^2 as the fiber, the metric 4.2 can be decomposed into two parts. We introduce coordinates (ν, r) on the cylindrical base M_Z , where ν serves as an angular coordinate on S^1 and r denotes the standard coordinate on \mathbb{R}^+ . The induced cylindrical metric on M_Z is then given by $g_z := -(\frac{2m}{r} - 1)d\nu^2 + 2d\nu dr$, while the metric on the hyperbolic plane H^2 is $g_{H^2} := d\theta^2 + \sinh^2(\theta)d\phi^2$, where (θ, ϕ) are pseudo-spherical polar coordinates.

Remark. Considering the universal covering space of the pseudo-Schwarzschild spacetime, we progressively recover flat space as $r \rightarrow \infty$. The metric, as given in Equation (4.2), exhibits a pathological behavior at $r = 2m$ and $r = 0$. As we will show later, $r = 2m$ corresponds to a Cauchy horizon, while $r = 0$ is a physical singularity analogous to the Schwarzschild singularity. However, there is a key difference: the pseudo-Schwarzschild singularity is timelike, whereas the Schwarzschild singularity is spacelike. This implies that no event inside the horizon can influence any event at $r > 2m$. A simple calculation reveals that $r = 0$ represents a curvature singularity, whereas the point $r = 2m$ is merely a coordinate singularity. Later, we will introduce appropriate coordinates that eliminate the coordinate singularity.

The pseudo-Schwarzschild spacetime is static inside the horizon and time-dependent outside of the horizon. For $r < 2m$, the t -direction ∂_t is timelike, and r is a spatial coordinate and the r -direction ∂_r is spacelike, as seen from the metric components:

$$g_{tt} = -\left(\frac{2m}{r} - 1\right) < 0$$

$$g_{rr} = \left(\frac{2m}{r} - 1\right)^{-1} > 0.$$

However, beyond the horizon, $r > 2m$, there is a reversal of the roles: t becomes a spatial coordinate and r becomes a timelike coordinate. In this region, the decrease of r signifies the passage of time. As long as you remain in the region $r > 2m$, you are inevitably moving forward in time and will hit the horizon at $r = 2m$. All trajectories lead inevitably to the horizon. Once you cross the horizon, the roles of t and r are effectively switched, with t becoming a timelike coordinate and r a spatial one.⁸ Analogous to the Schwarzschild metric, the pseudo-Schwarzschild metric has a horizon at $r = 2m$ and a singularity occurs at $r = 0$. As discussed earlier, the issue with our current coordinates becomes apparent along radial null geodesics, where the slope $\frac{dt}{dr}$ diverges as r converges towards $2m$, i.e. $\frac{dt}{dr} \rightarrow \infty$.

To eliminate the coordinate singularity at $r = 2m$, we can convert the pseudo-Schwarzschild coordinates into Eddington-Finkelstein coordinates. Similar to the Schwarzschild case, we set the term $r + 2m \ln |r - 2m|$

⁸We can analyze the behavior of radial null curves by setting $d\theta = d\phi = 0$ and studying the equation $dt = \pm \frac{1}{(\frac{2m}{r}-1)} dr$. For large r , the slope is $\frac{dt}{dr} = \pm 1$, which is consistent with the behavior in flat space. As we approach $r = 2m$, we get $\frac{dt}{dr} = \pm \infty$ meaning that the light cones close up at this point. Further, as we approach the singularity at $r = 0$, the light cones are stretched again, but are tilted according to their reversed role of t and r as timelike and spacelike coordinates.

equal to the tortoise coordinate r^* . Then, we set $\nu = -(t + r^*)$, which leads to the inverse relationship $t = -(\nu + r + 2m \ln |r - 2m|)$. Next, we take the derivative of this equation $dt = -d(\nu + r + 2m \ln |r - 2m|)$, and square both sides. By substituting this expression for dt^2 into the pseudo-Schwarzschild metric, we obtain the following form of the metric in terms of the tortoise coordinate

$$(4.3) \quad ds^2 = -\left(\frac{2m}{r} - 1\right)d\nu^2 + 2d\nu dr + r^2(d\theta^2 + \sinh^2(\theta)d\phi^2).$$

The new coordinate ν is periodic, with $0 \leq \nu < \beta$, similar to the previous coordinate t . A given point $(0, r, \theta, \phi)$ is identified with (b, r, θ, ϕ) , where b is the periodicity of the coordinate ν . These coordinates are naturally adapted to the null geodesics. Although the metric component $g_{\nu\nu}$ disappears at $r = 2m$, the coordinate transformation eliminates the singularity that existed at $r = 2m$ in the original pseudo-Schwarzschild coordinates. Moreover, the null hypersurface at $r = 2m$ serves as a Cauchy horizon, denoted H , and divides the spacetime M into two regions: M_2 , where $r < 2m$, and M_1 , where $r > 2m$. We can time-orient the manifold M by requiring that $-\partial_r$ be future-pointing. This leads to the conclusion that ∂_r is a lightlike vector throughout, ∂_ν is timelike for $r < 2m$, and spacelike for $r > 2m$.

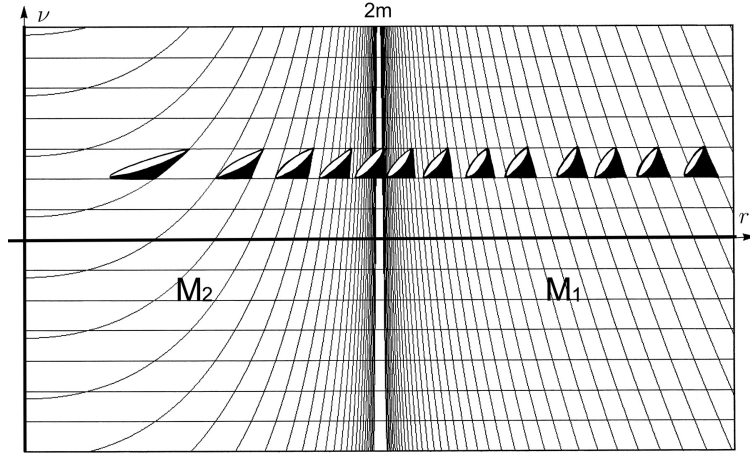


FIGURE 6. Pseudo-Schwarzschild spacetime in Eddington-Finkelstein coordinates.

Recalling that the pseudo-Schwarzschild spacetime is $M = M_Z \times_r H^2$, and its metric can be decomposed into the cylindrical metric g_Z and the hyperbolic metric g_{H^2} , we proceed by setting $\theta = \text{const}$ and $\phi = \text{const}$. Allowing ν and r to vary and take the values as previously defined, we obtain the 2-dimensional cylindrical pseudo-Schwarzschild spacetime $M_Z = S^1 \times \mathbb{R}^+$. This spacetime is described by the degenerate metric in Eddington-Finkelstein coordinates (see Figure 6):

$$(4.4) \quad g_Z := -\left(\frac{2m}{r} - 1\right)d\nu^2 + 2d\nu dr.$$

In two dimensions, the Christoffel symbols are identical for both the Schwarzschild and pseudo-Schwarzschild spacetimes. Therefore, the Riemann curvature tensor for the cylindrical pseudo-Schwarzschild spacetime (4.3) is given by $-R_{ttrr} = -\frac{2m}{r^3} =: K = \frac{1}{2}S$, where K denotes the Gaussian curvature and S represents the scalar

curvature. Since we require m to be non-negative and r to be positive, the Gaussian curvature is non-positive throughout the cylinder.⁹

4.1. Non-chronal region. In cylindrical coordinates (ν, r) , the ν -coordinate curves circle around the cylinder. Given the metric in Eddington-Finkelstein coordinates (as presented in Equation 4.4), besides θ, ϕ , we can also set r to a constant value and consider the one-dimensional line element

$$g_{\bar{Z}} = -\left(\frac{2m}{r} - 1\right)d\nu^2.$$

The curves $\gamma : [0, b] \rightarrow M$, defined by $\gamma(s) = (s, r, \theta, \phi)$, are closed because $\gamma(0) = (0, r, \theta, \phi) = (b, r, \theta, \phi) = \gamma(b)$. Since each curve is contained within a hypersurface of constant $r = \text{const}$ and is equipped with the metric $g_{\bar{Z}}$, the nature of the curves depends on the value of r : the curves are timelike if and only if $r < 2m$, the curves are spacelike if $r > 2m$. At $r = 2m$, the horizon H is null and consists of closed null curves $\gamma(s) = (s, 2m, \theta, \phi)$, where θ and ϕ are constant. Therefore, H serves as a chronology horizon for the closed orbits of constant r, θ, ϕ .

Proposition 4.1. *A curve $\gamma : I \rightarrow M_z$ with velocity $\gamma' = \gamma'_1 \partial_\nu + \gamma'_2 \partial_r$ is causal and future-pointing in M_1 if and only if $0 \leq \frac{2 \cdot \gamma'_2}{(\frac{2m}{r} - 1)} \leq \gamma'_1$, and is causal and future-pointing in M_2 if and only if $\frac{2 \cdot \gamma'_2}{(\frac{2m}{r} - 1)} \geq \gamma'_1 \geq 0$.*

Proof. We will not go into the details here, as the proof follows a similar structure to that of Lemma 6.2, where we discuss the properties of the pseudo-Reissner-Nordström spacetime. \square

Proposition 4.2. *There are no closed timelike curves in the region $M_1 \subset M_Z$.*

Proof. We begin by considering a foliation of M_Z using the hypersurfaces $\mathcal{H}_r := \{(\nu, r) \mid 0 \leq \nu \leq 2\pi\}$ where $r = \text{const}$. The hypersurfaces \mathcal{H}_r are spacelike for $r > 2m$, thus we have $M_1 = \bigcup_{r \in (2m, \infty)} \mathcal{H}_r$. Given that any curve in this region must be future-pointing, a curve in M_1 can only close up if it is contained within a circle in \mathcal{H}_r , i.e., if the curve is spacelike and satisfies the condition $r = \text{const}$. This is the only way for the curve to be periodic and contained within a single hypersurface \mathcal{H}_r . Therefore, such curves are spacelike. \square

The absence of closed timelike curves in region M_1 implicates that all closed timelike curves must be part of region M_2 .

4.2. Pseudo-Schwarzschild geodesics. The timelike geodesics for the pseudo-Schwarzschild spacetime in Eddington-Finkelstein coordinates are given by Equation (3.7), using the relation $g_{\nu\nu} = -(\frac{2m}{r} - 1)$:

$$(4.5) \quad \nu(r) = \int \frac{-\frac{1}{(\frac{2m}{r} - 1)} \left(\xi - \omega \sqrt{\xi^2 - (\frac{2m}{r} - 1)} \right)}{\omega \sqrt{\xi^2 - (\frac{2m}{r} - 1)}} dr = \int \frac{-1}{(\frac{2m}{r} - 1)} \left(\frac{\omega}{\sqrt{1 - \frac{(\frac{2m}{r} - 1)}{\xi^2}}} - 1 \right) dr.$$

There are two distinct sets of timelike geodesics in the pseudo-Schwarzschild spacetime. The first set corresponds to a timelike particle that penetrates the chronology horizon at $r = 2m$. This particle has a turning point at

⁹The Riemannian curvature tensor for the 4-dimensional pseudo-Schwarzschild spacetime can easily be computed by the prescription of Wick rotation and sign change.

$$r_{turn} = \frac{2m}{(\xi^2 + 1)},$$

which lies between the singularity and the chronology horizon. As a result, such a massive particle cannot reach the singularity. The second set of geodesics corresponds to a particle that spirals around the horizon as it approaches $r = 2m$, but it never crosses the horizon within this coordinate patch. For photons, the paths are determined by the equation

$$\nu(r) = \int \frac{-1}{\left(\frac{2m}{r} - 1\right)} (\omega - 1) dr.$$

Curiously, there is no obstruction for photons to fall into the singularity.

5. RELATION BETWEEN PSEUDO-SCHWARZSCHILD AND MISNER SPACETIME

We aim to investigate Misner space and the 2-dimensional pseudo-Schwarzschild spacetime (M_Z, g_Z) , focusing on similarities such as global causal structure, curvature, and geodesics. In addition to these, the conformal structure of these spacetimes is notably rich. A conformal transformation can sometimes convert a curved space with a non-zero Riemann tensor into a flat space with a zero Riemann tensor. However, depending on the dimension of the spacetime, a less strict concept of causal relatedness may be required. In this context, we introduce the concept of isocausality [6], which refers to a situation where the causal structure of spacetime may not be preserved globally under certain transformations, but the notion of causal relationships within specific regions remains consistent.

A glance at the causal structure of the cylindrical pseudo-Schwarzschild space and the 2-dimensional Misner space might suggest that the two associated metrics, metric (4.4) and the 2-dimensional variant of metric (2.3), are related. This raises the natural question of whether an isometric mapping exists between these manifolds. However, it is known that any isometry of a pseudo-Riemannian manifold preserves its curvature. Since the Riemann curvature vanishes in Misner space, but does not vanish in the cylindrical pseudo-Schwarzschild space, no isometry exists between them.

Remark 5.1. It is worth noting that in the special case $m = 0$, the 2-dimensional pseudo-Schwarzschild spacetime is defined on $S^1 \times \mathbb{R}$ and is flat. However, by setting $m = 0$, the chronology horizon in the pseudo-Schwarzschild space disappears, and closed timelike curves (CTCs) no longer exist. This distinction makes these spacetimes causally different, as the chronology horizon is a significant global feature that separates the chronology-violating region from the region without CTCs. In what follows, we will restrict our investigation to the case where $m > 0$.

5.1. General case. For radial trajectories in hyperbolically symmetric spacetimes, the geometry is effectively 1+1 dimensional. Therefore, for simplicity and ease of calculation, we first focus on the 2-dimensional Misner space and the cylindrical pseudo-Schwarzschild space, as these lead to relatively straightforward conformal transformations. Afterward, we turn our attention to 4-dimensional spacetimes, although the results from the 2-dimensional case cannot be directly generalized. This gives rise to an alternative perspective on causal equivalence, as introduced by [6]. This approach allows for the consideration of a much larger class of causally related spacetimes compared to the classical concept of conformally related spacetimes.

5.1.1. *Relation in the two-dimensional case.* Since the metrics under study are 2-dimensional, we know that both metrics in question belong to the same conformal equivalence class $[g]$ of conformally flat metrics.¹⁰ Hence, if the metrics $g_P, g_M \in [g]$ are both locally conformal to a flat metric g , i.e. $(g_M \sim g) \wedge (g_P \sim g)$, then by transitivity and symmetry we have $g_P \sim g_M$. As a result, we can locally transform the curved pseudo-Schwarzschild space with a non-vanishing Riemann tensor into the flat Misner space with a zero Riemann tensor by applying a conformal transformation.

Consider the 2-dimensional flat Misner space defined on $S^1 \times \mathbb{R}$ and equipped with the metric

$$(5.1) \quad ds^2 = Td\varphi^2 - dTd\varphi.$$

Remark 5.2. This version of Misner metric can be obtained from the 2-dimensional Minkowski metric (2.1) by the initial coordinate transformation $\tilde{t} = \eta \cosh(X_1)$ and $\tilde{x}_1 = \eta \sinh(X_1)$. This coordinate change results in the Misner metric $ds^2 = -d\eta^2 + \eta^2(dX_1)^2$, where $0 < \eta < \infty$, $0 \leq X_1 \leq 2\pi$. Another coordinate change with $\varphi = X_1 + \ln(\eta)$ and $T = \eta^2$ results in the Misner metric $-dTd\varphi + Td\varphi^2$, where the domains are $-\infty < T < \infty$ and $0 \leq \varphi \leq 2\pi$.

The pseudo-Schwarzschild spacetime is defined on $S^1 \times (0, \infty)$, with the corresponding line-element

$$(5.2) \quad ds^2 = -\left(\frac{2m}{r} - 1\right)d\nu^2 + 2d\nu dr.$$

Obviously the base manifolds are diffeomorphic. We start with Equation (5.2). For convenience, we introduce dimensionless quantities $\bar{r} = \frac{r}{m}$, $\bar{t} = \frac{t}{m}$ and rewrite the metric ((5.2)) as

$$\begin{aligned} ds^2 &= -\left(\frac{2}{\bar{r}} - 1\right)d(\bar{\nu}m)^2 + 2d(\bar{\nu}m)d(\bar{r}m) \\ &= m^2\left[-\left(\frac{2}{\bar{r}} - 1\right)d\bar{\nu}^2 + 2d\bar{\nu}d\bar{r}\right] \\ &= m^2\left(\frac{2}{\bar{r}} - 1\right)\left[-d\bar{\nu}^2 + \underbrace{2\left(\frac{2}{\bar{r}} - 1\right)^{-1}d\bar{r}d\bar{\nu}}_{d(r^*)}\right]. \end{aligned}$$

Next we introduce

$$(5.3) \quad d(r^*)^2 := 2\left(\frac{2}{\bar{r}} - 1\right)^{-1}d\bar{r},$$

with $r^* = -2(\bar{r} + 2 \log(\bar{r} - 2))$. This implies the line-element

$$ds^2 = m^2\left(\frac{2}{\bar{r}} - 1\right)\left[-d\bar{\nu}^2 + d(r^*)d\bar{\nu}\right].$$

We then redefine both coordinates as $\varphi = \alpha\bar{\nu}$ and $T = e^{\alpha r^*}$, where α is an arbitrary constant. Considering that $r^* = \frac{1}{\alpha} \cdot \log(T)$ yields

$$d\bar{\nu} = d\frac{\varphi}{\alpha} = \frac{1}{\alpha}d\varphi$$

¹⁰A metric is said to be conformally flat if it can be conformally transformed into a metric with vanishing Riemann curvature.

and

$$d(r^*) = d\left(\frac{1}{\alpha} \cdot \log(T)\right) = \frac{1}{\alpha T} dT.$$

With these expressions we obtain as line-element

$$\begin{aligned} ds^2 &= m^2\left(\frac{2}{\bar{r}} - 1\right)\left[-\left(\frac{1}{\alpha} d\varphi\right)^2 + \left(\frac{1}{\alpha T} dT\right)\left(\frac{1}{\alpha} d\varphi\right)\right] \\ &= m^2\left(\frac{2}{\bar{r}} - 1\right)\left[-\frac{1}{\alpha^2} d\varphi^2 + \frac{1}{\alpha^2 T} dT d\varphi\right]. \end{aligned}$$

By multiplication with (-1) we get

$$\begin{aligned} ds^2 &= -m^2\left(\frac{2}{\bar{r}} - 1\right)\frac{1}{\alpha^2} \frac{1}{T} [-Td\varphi^2 + dTd\varphi] = \underbrace{\left(\frac{2}{\bar{r}} - 1\right)\frac{m^2}{T\alpha^2}}_{\Omega(T)} [-dTd\varphi + Td\varphi^2] \\ &= \Omega(T)[-dTd\varphi + Td\varphi^2]. \end{aligned}$$

The conformal factor Ω is singular at the original horizon $r = 2m$. However, to ensure that the conformal factor is non-zero, we set the following expression for T (based on the defined terms above):

$$T = e^{\alpha r^*} = e^{\alpha(-2\bar{r} - 4 \log(\bar{r} - 2))} = e^{-2\alpha\bar{r}} \cdot e^{-\alpha 4 \log(2 - \bar{r})} = e^{-2\alpha\bar{r}} \cdot (2 - \bar{r})^{-4\alpha}.$$

Hence,

$$\begin{aligned} \Omega(\bar{r}) &= \left(\frac{2}{\bar{r}} - 1\right) \frac{m^2}{\alpha^2 (e^{-2\alpha\bar{r}} \cdot (2 - \bar{r})^{-4\alpha})} = \frac{m^2}{\bar{r}\alpha^2} (2 - \bar{r}) \frac{1}{(2 - \bar{r})^{-4\alpha}} \cdot e^{2\alpha\bar{r}} \\ &= \frac{m^2}{\bar{r}\alpha^2} (2 - \bar{r}) (2 - \bar{r})^{4\alpha} \cdot e^{2\alpha\bar{r}} = \frac{m^2 e^{2\alpha\bar{r}}}{\bar{r}\alpha^2} (2 - \bar{r})^{4\alpha+1}, \end{aligned}$$

and we choose $\alpha = -\frac{1}{4}$ to make Ω regular on the chronology horizon, e.g. to ensure $\Omega \neq 0$. Going back to the original coordinates, we have

$$\Omega(r) = \frac{m^2 e^{\frac{-r}{2m}}}{\frac{r}{16m}} \left(2 - \frac{r}{m}\right)^0 = \frac{16m^3 e^{\frac{-r}{2m}}}{r}$$

for the conformal factor. Furthermore, we rewrite the conformal factor in terms of the actual coordinates T , φ . Note that $r = \bar{r}m = 2m \left(W_n\left(-\frac{T}{2e}\right) + 1\right)$, $n \in \mathbb{Z}$, where the expression W is the *product log* function. Replacing r by $2m \left(W\left(-\frac{T}{2e}\right) + 1\right)$ yields the conformal factor

$$\begin{aligned} \Omega(T) &= \frac{16m^3 e^{\frac{-r}{2m}}}{r} = \frac{16m^3 e^{-\frac{2m \left(W\left(-\frac{T}{2e}\right) + 1\right)}{2m}}}{2m \left(W\left(-\frac{T}{2e}\right) + 1\right)} = \frac{8m^2 e^{-\left(W\left(-\frac{T}{2e}\right) + 1\right)}}{\left(W\left(-\frac{T}{2e}\right) + 1\right)} \\ &= \frac{8m^2 e^{-\left(W\left(-\frac{T}{2e}\right) + 1\right)}}{W\left(-\frac{T}{2e}\right) + 1} = \frac{8m^2}{e^{\left(W\left(-\frac{T}{2e}\right) + 1\right)} \cdot W\left(-\frac{T}{2e}\right) + 1} = \frac{8m^2}{e^{\left(W\left(-\frac{T}{2e}\right) + 1\right)} - \frac{T}{2}} \end{aligned}$$

and the corresponding line-element

$$ds^2 = \frac{8m^2}{\underbrace{e^{(W(-\frac{T}{2c})+1)} - \frac{T}{2}}_{\Omega(T)}} [-dTd\varphi + Td\varphi^2],$$

where the conformal factor, $\Omega(T)$, is a smooth, non-zero scalar function of the spacetime coordinates. Conformal transformations preserve the local causal structure: they map timelike curves to timelike curves, spacelike curves to spacelike curves, and null curves to null curves. Furthermore, we have the well-known

Proposition 5.3. *Conformal transformations between 2-dimensional Lorentzian manifolds send null hypersurfaces to null hypersurfaces and therefore null geodesics to null geodesics.*

However, timelike geodesics in one spacetime are not necessarily geodesics in another conformally equivalent spacetime, even if both spacetimes are related by a conformal diffeomorphism. Nonetheless, the treatments of timelike geodesics in Equation 2.2 and Equation 4.2 demonstrate that the geodesic behavior in both spacetimes is, in fact, similar.

This means that for the 1 + 1 dimensional pseudo-Schwarzschild and Misner spacetimes, we can identify conformal transformations and demonstrate that timelike geodesics are of a similar type in both spacetimes. This establishes a notable relationship between them, with the 2-dimensional pseudo-Schwarzschild spacetime being viewed as a modification or generalization of Misner space. However, the 4-dimensional pseudo-Schwarzschild solution is not conformally flat, as indicated by the non-zero components of the conformally invariant Weyl tensor. In fact, only one independent spin component of the Weyl tensor does not vanish, specifically the Weyl scalar $C = \frac{m}{r^3}$. Therefore, in this context, a less strict definition of causal relatedness is required.

5.1.2. *Relation in the 4-dimensional case.* Since the Weyl curvature tensor vanishes identically in two dimensions, all 2-dimensional Lorentz metrics belong to the same conformal class of flat metrics. Therefore, it is relatively straightforward to find conformal transformations between any two representatives of this conformal class. In dimensions greater than three, the Weyl curvature tensor is generally non-zero, and a necessary condition for a spacetime to be conformally flat is that the Weyl tensor vanishes. As a result, establishing an explicit conformal relation between 4-dimensional spacetimes becomes significantly more challenging.

In four dimensions, Misner space is flat, while pseudo-Schwarzschild spacetime is not conformally flat. Therefore, these two spacetimes do not belong to the same conformal class. At this point, we turn to the concept of causal relations, known as isocausality, which is more general than conformal relations. We consider mappings that preserve causal relations, even if their inverses do not necessarily do so. This notion was proposed by García-Parrado and Senovilla [6] and further developed by A. García-Parrado and M. Sánchez [7]. The analogy between the pseudo-Schwarzschild and Misner spacetimes becomes clearer through Penrose diagrams, as shown in Figure 7. These diagrams reveal that the universal covering spaces of these spacetimes share the same large-scale structure.

Remark 5.4. The boundaries in the diagram are not part of the original spacetimes. It is important to remember that we imposed periodicity on one coordinate in the original spacetimes, which cannot be appropriately represented in the Penrose diagrams.

In earlier work [18] we conjectured that the 4-dimensional pseudo-Schwarzschild spacetime and Misner space are isocausal. In the present paper, we prove this result and extend it to include the pseudo-Reissner-Nordström spacetime. The proof, given in Proposition 7.1, establishes that all three models are pairwise isocausal on their universal covers and on suitable causally regular regions of the compactified spacetimes, and provides explicit criteria for when this equivalence descends globally.

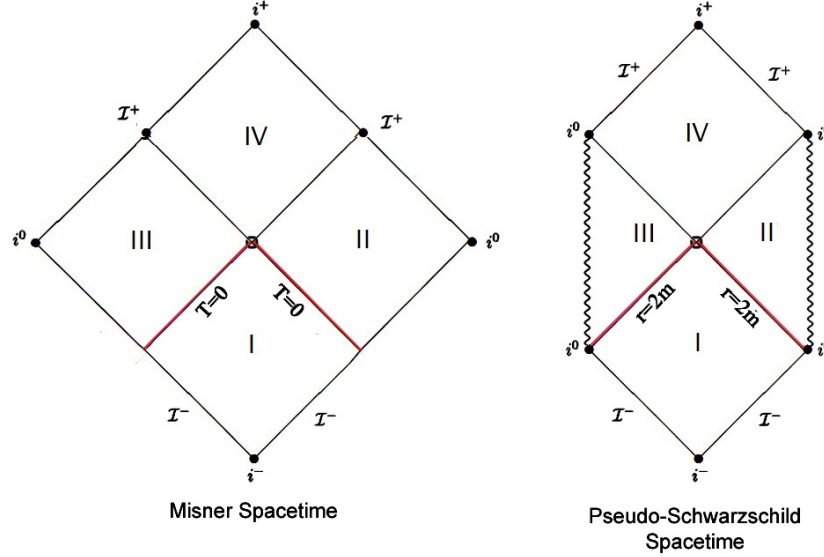


FIGURE 7. Conformal diagrams for the coverings spaces of Misner space and pseudo-Schwarzschild spacetime. The resemblance is noteworthy and we suspect a causal relationship. According to [6], Penrose diagrams are very helpful to get a clearer picture of the large-scale structure and to detect isocausality.

6. PSEUDO-REISSNER-NORDSTRÖM SPACETIME

We begin with the well-known Reissner-Nordström spacetime and modify it to create a novel spacetime, which we refer to as the pseudo-Reissner-Nordström spacetime. The two metrics are related through Wick rotation and a change in signature. Comprehensive references for the Reissner-Nordström spacetime include [2, 11, 15]. Our focus will be on the geometry of the newly derived pseudo-Reissner-Nordström spacetime, examining its global structure, geodesics, and causal properties. Furthermore, we will explore how this spacetime relates to the pseudo-Schwarzschild and Misner spacetimes, with many of the properties we derive also applying to these two spacetimes.

By performing a Wick rotation $\theta \rightarrow i\theta$ on the Reissner-Nordström metric, changing the range of θ from $[0, \pi]$ to $[0, +\infty]$, flipping the signature, and identifying $t + P$ with t , we obtain the manifold

$$M := S^1 \times (0, \infty) \times H_r^2,$$

with coordinates (t, r, θ, φ) , equipped with the metric

$$(6.1) \quad ds^2 = -\left(\frac{2m}{r} - \frac{q^2}{r^2} - 1\right)dt^2 + \left(\frac{2m}{r} - \frac{q^2}{r^2} - 1\right)^{-1}dr^2 + r^2(d\theta^2 + \sinh^2(\theta)d\phi^2).$$

Similar to the pseudo-Schwarzschild manifold, the 1-sphere S^1 (with $0 \leq t < t + \alpha$) is topologically equivalent to an interval with its endpoints identified. The surface H_r^2 is 2-dimensional and corresponds to the upper sheet of a two-sheeted spacelike hyperboloid. The coordinate θ can take any positive value, while ϕ is periodic and ranges from $0 \leq \phi < 2\pi$. The real constants m and q represent mass and electric charge, respectively, and are assumed to be positive. This new metric can also be derived by performing a Wick rotation and a signature change on the Schwarzschild metric, followed by the substitution

$$m \rightarrow m(r) := m - \frac{q^2}{2r},$$

which reduces back to the pseudo-Schwarzschild metric when $q = 0$. The metric, as given in Equation (5), is singular when

$$\frac{2m}{r} - \frac{q^2}{r^2} - 1 = 0 \iff r_{\pm} = m \pm \sqrt{m^2 - q^2},$$

and also at $r = 0$.

The singularities at $r = r_-$ and $r = r_+$ are not true physical singularities; rather, they represent quasi-regular singularities arising from geodesic incompleteness.

Remark. The Reissner-Nordström spacetime is not a vacuum solution of Einstein's field equations, as it contains matter in the form of an electromagnetic field. It is instead an *electrovacuum* solution of the Einstein-Maxwell equations, described by an energy-momentum tensor $T_{\mu\nu}$ sourced by the electromagnetic field (from a vector potential). The metric, with signature $(-+++)$, satisfies the Einstein equations in the form $G_{\mu\nu} = R_{\mu\nu} - \frac{1}{2}Rg_{\mu\nu} = \kappa T_{\mu\nu}$, where $T_{\mu\nu}$ is the energy-momentum tensor of the electromagnetic field.

Our construction of the pseudo-Reissner-Nordström spacetime begins by performing a Wick rotation on the angular coordinate, $\theta \rightarrow i\theta$, followed by a sign reversal of the metric tensor, $g'_{\mu\nu} = -g_{\mu\nu}$. This transformation results in a hyperbolic geometry in the angular sector. While the Einstein tensor $G_{\mu\nu}$ remains invariant under this sign reversal, the energy-momentum tensor, which is constructed from the metric, changes sign such that $T'_{\mu\nu} = -T_{\mu\nu}$. Consequently, the field equations for the new metric become $G_{\mu\nu} = \kappa T'_{\mu\nu} = -\kappa T_{\mu\nu}$.

This resulting spacetime is no longer a solution of the standard Einstein-Maxwell equations. The gravitational source now corresponds to an energy-momentum tensor that violates the weak energy condition, as indicated by $T_{\mu\nu}k^{\mu}k^{\nu} < 0$ for some timelike vector k^{μ} . This violation implies the presence of a source of *exotic matter* with negative energy density. This situation differs significantly from the pseudo-Schwarzschild metric, which remains a valid vacuum solution because its original stress-energy tensor was zero and remains so after the analogous transformation.

This distinction is critical. While the Misner and pseudo-Schwarzschild spacetimes are both vacuum solutions, the pseudo-Reissner-Nordström spacetime is a non-vacuum solution that requires exotic matter. This non-vacuum character is what makes it a particularly surprising and significant member of the family of causality-violating spacetimes we are investigating.

Before discussing causality, we will change coordinates and define the extended manifold. There exists a set of coordinates that better describe the singularities at $r = r_-$ and $r = r_+$. To achieve this, we introduce the Eddington-Finkelstein coordinates (ν, r, θ, ϕ) , which can be introduced as follows:

We regard θ and ϕ being constant and first compute the tortoise coordinate r^* by setting

$$ds^2 = -\left(\frac{2m}{r} - \frac{q^2}{r^2} - 1\right)dt^2 + \frac{1}{-\left(\frac{2m}{r} - \frac{q^2}{r^2} - 1\right)}dr^2 = 0.$$

We can now assert that

$$\frac{dt^2}{dr^2} = \frac{1}{\left(\frac{2m}{r} - \frac{q^2}{r^2} - 1\right)^2} \implies \frac{dt}{dr} = \pm \frac{1}{\left(\frac{2m}{r} - \frac{q^2}{r^2} - 1\right)}.$$

Then we integrate $\frac{dt}{dr} = \frac{1}{\left(\frac{2m}{r} - \frac{q^2}{r^2} - 1\right)}$ to obtain

$$\begin{aligned} t(r) &= \int \frac{1}{\left(\frac{2m}{r} - \frac{q^2}{r^2} - 1\right)} dr \\ &= (2m^2 - q^2) \cdot \tan^{-1}\left(\frac{r-m}{\sqrt{q^2 - m^2}}\right) - m \cdot \log(-2mr - q^2 + r^2) - r + c, \end{aligned}$$

which yields the tortoise coordinate which is defined by

$$r^* := (2m^2 - q^2) \cdot \tan^{-1}\left(\frac{r-m}{\sqrt{q^2 - m^2}}\right) - m \cdot \log(-2mr - q^2 + r^2) - r.$$

Thus, we obtain the Eddington-Finkelstein coordinates $\nu = t + r^*$. Our next step is to express the pseudo-Reissner-Nordström metric in terms of the tortoise coordinate. We define $t = \nu - r^*$ and substitute t with the term $\nu - r^*$ in the original metric (6.1):

$$\begin{aligned}
ds^2 &= -\left(\frac{2m}{r} - \frac{q^2}{r^2} - 1\right) (d(\nu - r*))^2 + \left(\frac{2m}{r} - \frac{q^2}{r^2} - 1\right)^{-1} dr^2 + r^2(d\theta^2 + \sinh^2(\theta)d\phi^2) \\
&= -\left(\frac{2m}{r} - \frac{q^2}{r^2} - 1\right) \left(\underbrace{\frac{\partial(\nu - r*)}{\partial r}}_{\left(\frac{2m}{r} - \frac{q^2}{r^2} - 1\right)^{-1}} dr + \underbrace{\frac{\partial(\nu - r*)}{\partial \nu}}_1 d\nu \right)^2 \\
&\quad + \left(\frac{2m}{r} - \frac{q^2}{r^2} - 1\right)^{-1} dr^2 + r^2(d\theta^2 + \sinh^2(\theta)d\phi^2) \\
&= -\left(\frac{2m}{r} - \frac{q^2}{r^2} - 1\right) \left[\left(\frac{1}{\left(\frac{2m}{r} - \frac{q^2}{r^2} - 1\right)^2}\right) dr^2 - 2 \cdot 1 \cdot \frac{1}{\left(\frac{2m}{r} - \frac{q^2}{r^2} - 1\right)} dr d\nu + 1 d\nu^2 \right] \\
&\quad + \left(\frac{2m}{r} - \frac{q^2}{r^2} - 1\right)^{-1} dr^2 + r^2(d\theta^2 + \sinh^2(\theta)d\phi^2) \\
&= -\left(\frac{2m}{r} - \frac{q^2}{r^2} - 1\right)^{-1} dr^2 + 2drd\nu - \left(\frac{2m}{r} - \frac{q^2}{r^2} - 1\right) d\nu^2 \\
&\quad + \left(\frac{2m}{r} - \frac{q^2}{r^2} - 1\right)^{-1} dr^2 + r^2(d\theta^2 + \sinh^2(\theta)d\phi^2) \\
&= -\left(\frac{2m}{r} - \frac{q^2}{r^2} - 1\right) d\nu^2 + 2drd\nu + r^2(d\theta^2 + \sinh^2(\theta)d\phi^2).
\end{aligned}$$

Hence, in terms of the Eddington-Finkelstein coordinates, the metric takes the form

$$(6.2) \quad ds^2 = -\left(\frac{2m}{r} - \frac{q^2}{r^2} - 1\right) d\nu^2 + 2drd\nu + r^2(d\theta^2 + \sinh^2(\theta)d\phi^2),$$

where ν has the same periodicity as t . The metric is now regular at $r = r_-$ and $r = r_+$, but we still have an irremovable singularity at $r = 0$. Fortunately, the first two terms are independent of the coordinates θ and ϕ . To align the pseudo-Reissner Nordström spacetime with the other examples discussed in this article, and because most of our calculations only apply to the coordinates ν and r , we can ignore the term $r^2(d\theta^2 + \sinh^2(\theta)d\phi^2)$. From now on we treat θ and ϕ as constants and consider the cylindrical metric

$$(6.3) \quad ds^2 = -\left(\frac{2m}{r} - \frac{q^2}{r^2} - 1\right) d\nu^2 + 2drd\nu,$$

with ν being periodic with period α , i.e., the metric is defined on $M := S^1 \times (0, \infty)$. Although we have removed the coordinate singularities, the light cones still tilt over at $r = r_{\pm}$, as we will discuss later. The horizon function $H(r)$ given by

$$H(r) = \frac{2m}{r} - \frac{q^2}{r^2} - 1$$

determines the horizons at $r = r_{\pm}$. In contrast to the pseudo-Schwarzschild spacetime, there are three distinct cases:

(i) For $m > q$, there are two horizons: The event horizon, which is also a Cauchy horizon, at

$$r = r_- = m - \sqrt{m^2 - q^2},$$

and a Cauchy horizon at

$$r = r_+ = m + \sqrt{m^2 - q^2}.$$

Above all, both horizons are chronology horizons.

(ii) For $m = q$, there is single horizon at

$$r = r_+ = r_- = m = q,$$

which serves as both a Cauchy horizon and an event horizon.

(iii) For $m < q$, no horizon exists, which in the Reissner-Nordström spacetime results in a *naked singularity* observable from the outside. Although an event horizon is absent, the future singularity at $r = 0$ remains spacelike and thus remains hidden from external observers. This scenario parallels the pseudo-Schwarzschild solution with negative mass, a topic we will not explore further here.

The Riemann curvature tensor for the 2-dimensional pseudo-Reissner-Nordström spacetime can be obtained using the same approach as in Section 4 for the pseudo-Schwarzschild case. The scalar curvature then follows immediately

$$S = g^{jl} Ric_{jl} = \sum_{jl} g^{jl} Ric_{jl} = -2 \cdot \frac{2mr - 3q^2}{r^4}.$$

Thus, the Gaussian curvature K is given by

$$K = \frac{1}{2}S = -\frac{2mr - 3q^2}{r^4} = -R_{1212}.$$

This result confirms that the Gaussian curvature changes sign based on the value of r : for $r < \frac{3q^2}{2m}$, we find $2mr - 3q^2 < 0$, making the Gaussian curvature $K > 0$. Conversely, for $r > \frac{3q^2}{2m}$, we have $2mr - 3q^2 > 0$, resulting in $K < 0$.

To obtain the curvature for the 4-dimensional case, we can derive the Riemann curvature tensor for the pseudo-Reissner-Nordström spacetime by applying a Wick rotation to the well-known Reissner-Nordström spacetime. This approach uses the established properties of the Reissner-Nordström solution, allowing us to modify the spacetime signature and adapt the curvature properties for the pseudo-Reissner-Nordström framework.

6.1. Pseudo-Reissner-Nordström spacetime with two horizons. The pseudo-Reissner-Nordström spacetime $M = S^1 \times (0, \infty)$ with $m > q$ and two horizons at $r = r_{\pm}$ presents a particularly interesting configuration. These horizons divide M into three distinct regions: $M_3 = \{(\nu, r) \in M \mid 0 < r < r_-\}$, $M_2 = \{(\nu, r) \in M \mid r_- < r < r_+\}$, and $M_1 = \{(\nu, r) \in M \mid r_+ < r < \infty\}$. In analogy with the pseudo-Schwarzschild spacetime, the coordinate vector field ∂_r is null, with $-\partial_r$ designated as future-pointing (indicating that r decreases as one moves from past to future). The behavior of the vector field ∂_ν varies across regions: it is spacelike in M_1 , timelike in M_2 , and again spacelike in M_3 .

For radial null geodesics, we first set

$$ds^2 = -\left(\frac{2m}{r} - \frac{q^2}{r^2} - 1\right) d\nu^2 + 2drd\nu = 0,$$

from which we immediately see

$$\frac{d\nu}{dr} = \begin{cases} 2\left(\frac{2m}{r} - \frac{q^2}{r^2} - 1\right)^{-1} & (\text{outgoing}) \\ 0 & (\text{infalling}) \end{cases}.$$

In the next step we consider the outgoing radial null curves

$$d\nu = \frac{2}{-1 + \frac{2m}{r} - \frac{q^2}{r^2}} dr = \frac{2r^2}{R} dr = \frac{2r^2}{cr^2 + br + a} dr,$$

where $R = 2mr - q^2 - r^2$, $a = -q^2$, $b = 2m$ and $c = -1$. This then takes the form of the integral $\nu(r) = 2 \int \frac{r^2}{R} dr = 2(-r - m \ln R + (2m^2 - q^2) \int \frac{1}{R} dr)$, where $\Delta = 4ac - b^2 = 4(q^2 - m^2) < 0$, and

$$\int \frac{1}{R} dr = \frac{1}{\sqrt{-\Delta}} \ln \frac{\sqrt{-\Delta} - (b + 2cr)}{(b + 2cr) + \sqrt{-\Delta}} = \frac{1}{\sqrt{-4(q^2 - m^2)}} \ln \frac{\sqrt{-4(q^2 - m^2)} - (2m - 2r)}{(2m - 2r) + \sqrt{-4(q^2 - m^2)}}.$$

From this we obtain $\nu = \text{const}$ and

$$\nu(r) = 2 \left(-r - m \ln(2mr - q^2 - r^2) + (2m^2 - q^2) \left(\frac{1}{\sqrt{-4(q^2 - m^2)}} \ln \frac{\sqrt{-4(q^2 - m^2)} - (2m - 2r)}{(2m - 2r) + \sqrt{-4(q^2 - m^2)}} \right) \right).$$

Consequently, for large r , the slope of the light cones is $\frac{d\nu}{dr} = \begin{cases} -2 \\ 0 \end{cases}$, while as we approach r_+ , the slope becomes $\frac{d\nu}{dr} = \begin{cases} \rightarrow -\infty \\ 0 \end{cases}$, and the light cones begin to open up once we cross the horizon (as illustrated in Figure 8). As we move closer to r_- , the light cones close up, giving $\frac{d\nu}{dr} = \begin{cases} \rightarrow +\infty \\ 0 \end{cases}$. We can traverse this horizon, and as the light cones tilt over, approaching the singularity at $r = 0$, the slope becomes $\frac{d\nu}{dr} = \begin{cases} 0 \\ 0 \end{cases}$.

In regions M_3 and M_1 , future-pointing paths move in the direction of decreasing r , while in region M_2 this behavior conflicts with causality. The surfaces at $r = r_{\pm}$ act as both chronology horizons and event horizons; crossing these horizons signifies a point of no return. For a particle initially starting its journey in region M_1 , encountering the horizon at $r = r_+$ is inevitable, while it is possible to accelerate away from the horizon at $r = r_-$.

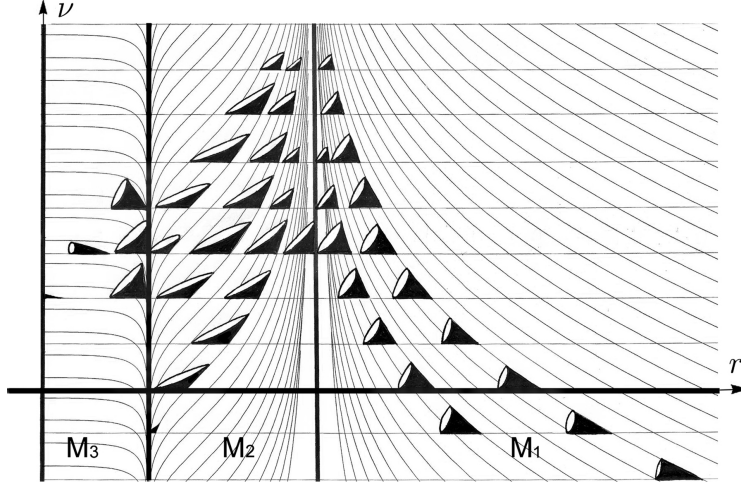


FIGURE 8. Spacetime diagram for the pseudo-Reissner-Nordström spacetime with two horizons.

6.1.1. Non-chronal region M_2 . Although the closed timelike curves (CTCs) in this case primarily arise from the periodicity of the ν -coordinate, the tilting of light cones also contributes to the formation of CTCs.

Claim 6.1. A causal curve $\gamma : I \rightarrow M$ with velocity $\gamma' = \gamma'_1 \partial_\nu + \gamma'_2 \partial_r$ is future-pointing if and only if $\gamma'_1 \geq 0$.

Proof. The inner product of two future-pointing causal vectors is non-positive. We already defined $-\partial_r$ to be future-pointing, thus the claim follows directly from $0 \geq g(\gamma', -\partial_r) = -\gamma'_1 \iff \gamma'_1 \geq 0$. \square

Claim 6.2. A curve $\gamma : I \rightarrow M$ with velocity $\gamma' = \gamma'_1 \partial_\nu + \gamma'_2 \partial_r$ is causal and future-pointing in M_2 if and only if $\frac{2 \cdot \gamma'_2}{(\frac{2m}{r} - \frac{q^2}{r^2} - 1)} \leq \gamma'_1$. In M_1 and M_3 , it is causal and future-pointing if and only if $\frac{2 \cdot \gamma'_2}{(\frac{2m}{r} - \frac{q^2}{r^2} - 1)} \geq \gamma'_1 \geq 0$.

Proof. A future-pointing causal curve is a curve $\gamma : I \rightarrow M$ satisfying that $g(\gamma', \gamma') \leq 0$ and $\gamma'_1 \geq 0$. Hence,

$$\begin{aligned} 0 \geq g(\gamma', \gamma') &= g(\gamma'_1 \partial_\nu + \gamma'_2 \partial_r, \gamma'_1 \partial_\nu + \gamma'_2 \partial_r) = \gamma'_1 [2 \cdot \gamma'_2 - \gamma'_1 \cdot (\frac{2m}{r} - \frac{q^2}{r^2} - 1)] \\ \iff 2 \cdot \gamma'_2 - \gamma'_1 \cdot (\frac{2m}{r} - \frac{q^2}{r^2} - 1) &\leq 0 \iff 2 \cdot \gamma'_2 \leq \gamma'_1 \cdot (\frac{2m}{r} - \frac{q^2}{r^2} - 1). \end{aligned}$$

Now we have to discriminate between two cases:

- i) $r_- < r < r_+ \implies (\frac{2m}{r} - \frac{q^2}{r^2} - 1) > 0: \frac{2 \cdot \gamma'_2}{(\frac{2m}{r} - \frac{q^2}{r^2} - 1)} \leq \gamma'_1$
- ii) $0 < r < r_- \vee r_+ < r \implies (\frac{2m}{r} - \frac{q^2}{r^2} - 1) < 0: \frac{2 \cdot \gamma'_2}{(\frac{2m}{r} - \frac{q^2}{r^2} - 1)} \geq \gamma'_1,$

and this is precisely the assertion of the claim. \square

The primary significance of this result lies in its identification of regions where closed timelike curves (CTCs) may occur, thereby justifying a focus on region M_2 . The earlier identification of $\nu = 0$ and $\nu = \alpha$ leads directly to this outcome. On the hypersurfaces H_r , where $r = \text{const}$, the metric reduces to

$$g_{H_r} = -\left(\frac{2m}{r} - \frac{q^2}{r^2} - 1\right)d\nu^2,$$

which means that these surfaces are unconditionally spacelike when $0 < r < r_- \vee r_+ < r$. For a fixed value of r , the circle of constant radius $\gamma_r = \{(\nu, r) \mid 0 \leq \nu \leq \alpha\}$ is timelike if $r_- < r < r_+$, spacelike if $0 < r < r_- \vee r_+ < r$, and null for $r = r_{\pm}$. This implies that a curve $\gamma(s) = (s, r)$ with constant $r \in (r_-, r_+)$ forms a closed timelike curve due to the periodicity of ν , and when $r = r_{\pm}$, it forms a closed lightlike curve. Thus, we refer to $r = r_{\pm}$ as the chronology horizon, and we designate the surfaces $H_- := \{(\nu, r_-) \mid 0 \leq \nu \leq P\}$ and $H_+ := \{(\nu, r_+) \mid 0 \leq \nu \leq P\}$, with constant radii r_- and r_+ , respectively, as the null hypersurfaces.

Proposition 6.3. *A closed timelike curve in M must lie entirely within region M_2 .*

Proof. From what has already been proved, for a timelike future-pointing curve in M_1 we have the requirement $\frac{2}{\left(\frac{2m}{r} - \frac{q^2}{r^2} - 1\right)} < \frac{\gamma'_1}{\gamma'_2}$. The procedure is to exclude that a timelike curve starts in region M_1 , enters the region M_2 and loops back to its initial point in M_1 . Let us consider a timelike, future-pointing curve $\gamma : [0, 1] \rightarrow M$ starting in M_1 . The tangent vector to the curve is given by $\gamma' = \gamma'_1 \partial_\nu + \gamma'_2 \partial_r$, where γ'_1 and γ'_2 are the components of the tangent vector. Since the fundamental vector field ∂_r is null everywhere, and given that γ is future-pointing and timelike, we have $\gamma'_1 > 0$ along the entire curve γ , and $\gamma'_2 < 0$ for $\gamma \subset M_1$.

Assume $\gamma(0) \in M_1$, then $\frac{2}{\underbrace{\left(\frac{2m}{r} - \frac{q^2}{r^2} - 1\right)}_{< 0}} < \frac{\gamma'_1}{\gamma'_2}$ follows from the foregoing Lemma. As we approach the

Cauchy horizon H_+ at r_+ , we have $\left(\frac{2m}{r} - \frac{q^2}{r^2} - 1\right) \rightarrow 0$, and thus $\frac{2}{\left(\frac{2m}{r} - \frac{q^2}{r^2} - 1\right)} \rightarrow -\infty$. Consequently, $-\infty < \frac{\gamma'_1}{\gamma'_2}$ as we approach H_+ . The curve would remain in M_1 and not enter region M_2 only if $\gamma'_2 = 0$, meaning that it would be tangent to ∂_ν and thus lightlike. However, since γ is timelike and $\gamma'_2 \neq 0$, it follows that the curve must enter the region M_2 .

In region M_2 , we have the requirement $\gamma'_2 < \frac{\gamma_1 \cdot \left(\frac{2m}{r} - \frac{q^2}{r^2} - 1\right)}{2}$. As $r \rightarrow r_+$, we observe that $\frac{\gamma_1 \cdot \left(\frac{2m}{r} - \frac{q^2}{r^2} - 1\right)}{2} \rightarrow 0$, and thus we can assert that $\gamma'_2 < 0$ close to the horizon H_+ . This shows that γ cannot cross the horizon H_+ anymore and is therefore confined to region M_2 . Consequently, γ cannot return to its initial position. In particular, it is evident that there are no closed timelike curves (CTCs) in region M_1 , and similar considerations apply to region M_3 .

It is immediately clear that a curve $\gamma(s) = (s, r)$ with constant $r \in (r_-, r_+)$ forms a closed timelike curve. According to Proposition 2.1, there are infinitely many CTCs in region M_2 . \square

The above arguments establish the following

Corollary 6.4. *There are closed timelike curves in M_2 , and for every point $p \in M_2$, there exists a closed timelike curve passing through p .*

Proof. Under the conditions stated above, consider $\gamma : [0, L] \rightarrow M, \gamma(s) = (ks, r), k \geq 0$. \square

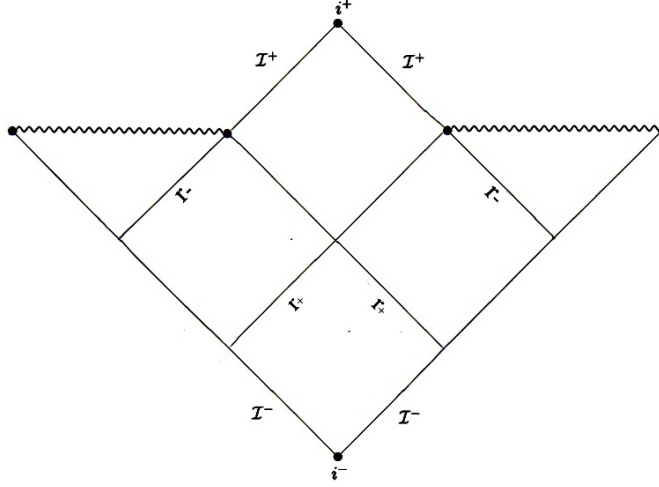


FIGURE 9. Conformal diagram for the pseudo-Reissner-Nordström spacetime with two horizons.

6.2. Extremal pseudo-Reissner-Nordström spacetime. The extremal 2-dimensional pseudo-Reissner-Nordström spacetime M with $m = q$ has only one horizon at $r = m$, which separates M into two regions: $M_3 = \{(\nu, r) \in M \mid 0 < r < m\}$ and $M_2 = \{(\nu, r) \in M \mid m < r\}$. As before, we time-orient M by requiring $-\partial_r$ to be future pointing. The metric degenerates to

$$ds^2 = -\left(\frac{2m}{r} - \frac{m^2}{r^2} - 1\right)d\nu^2 + 2drd\nu = \left(\frac{m^2 - 2mr + r^2}{r^2}\right)d\nu^2 + 2drd\nu = \frac{(m-r)^2}{r^2}d\nu^2 + 2drd\nu.$$

The Gaussian curvature is

$$K = \frac{1}{2}S = -\frac{m(2r - 3m)}{r^4} = -R_{trtr},$$

where for $r < \frac{3m}{2}$, we have $2mr - 3m^2 < 0$, so the Gaussian curvature is $\frac{2mr-3m^2}{r^4} > 0$, and for $r > \frac{3m}{2}$, the curvature becomes negative.

By the same method as in Subsection 6.1, we calculate the radial null geodesics by setting

$$ds^2 = -\left(\frac{2m}{r} - \frac{m^2}{r^2} - 1\right)d\nu^2 + 2drd\nu = 0,$$

and we obtain

$$\frac{d\nu}{dr} = \begin{cases} 2\left(\frac{2m}{r} - \frac{m^2}{r^2} - 1\right)^{-1} & (\text{outgoing}) \\ 0 & (\text{infalling}) \end{cases}.$$

This term can be handled in much the same way as in Section 6.1, the only difference being that $q = m$. A quick verification shows that we obtain the integral $\nu = \text{const}$, and the expression for $\nu(r)$ is

$$\nu(r) = 2 \left(-r + 2m \ln(r - m) - \frac{m^2}{m - r} \right).$$

Since $g(\partial_r, \partial_r) = 0$ for all $r \in (0, \infty)$, we conclude that ∂_r is lightlike. Additionally, from $g(\partial_u, \partial_u) = \frac{(m-r)^2}{r^2} > 0$ for all $r \in (0, \infty)$, we can deduce that ∂_u is spacelike at any point $p \in M$. See Figure 10.

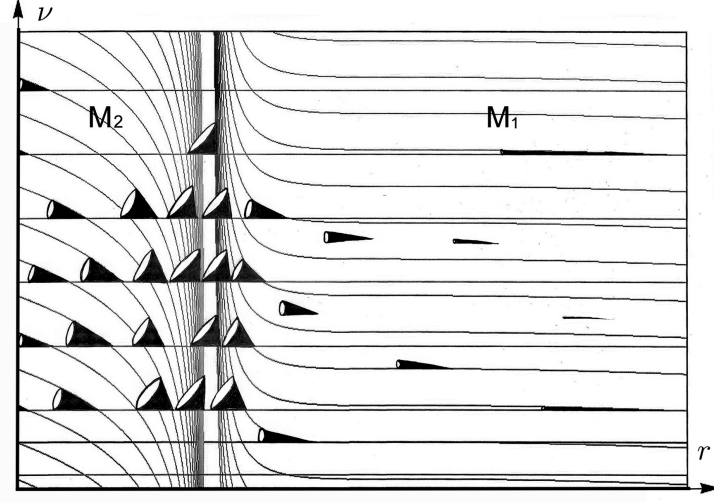


FIGURE 10. Light cone structure for the extremal pseudo-Reissner-Nordström spacetime.

Proposition 6.5. *A curve $\gamma : I \rightarrow M$ with velocity $\gamma' = \gamma'_1 \partial_\nu + \gamma'_2 \partial_r$ is causal and future-pointing in M if and only if $2 \cdot \gamma'_2 \leq -\gamma'_1 \cdot \frac{(m-r)^2}{r^2}$.*

Proof. A future-pointing causal curve is a curve $\gamma : I \rightarrow M$, satisfying that $g(\gamma', \gamma') \leq 0$ and $\gamma'_1 \geq 0$. Hence,

$$\begin{aligned} 0 \geq g(\gamma', \gamma') &= g(\gamma'_1 \partial_\nu + \gamma'_2 \partial_r, \gamma'_1 \partial_\nu + \gamma'_2 \partial_r) = \gamma'_1 [2 \cdot \gamma'_2 + \gamma'_1 \cdot \frac{(m-r)^2}{r^2}] \\ \iff 2 \cdot \gamma'_2 + \gamma'_1 \cdot \frac{(m-r)^2}{r^2} &\leq 0 \iff 2 \cdot \gamma'_2 \leq \underbrace{-\gamma'_1 \cdot \frac{(m-r)^2}{r^2}}_{\leq 0}. \end{aligned}$$

□

We are now in the position to show

Proposition 6.6. *All future pointing causal curves in M_2 converge towards the singularity $r = 0$.*

Proof. For a causal future-pointing curve $\gamma : [0, 1] \rightarrow M_2 : s \mapsto \gamma(s)$ we have the requirement $\gamma_1 \geq 0$, and $\gamma'_2 \leq \underbrace{-\gamma'_1 \cdot \frac{(m-r)^2}{r^2} \cdot \frac{1}{2}}_{\leq 0} \implies \gamma'_2 \leq 0$. For $\gamma'_2 = 0$ we have $0 \leq \underbrace{-\gamma'_1 \cdot \frac{(m-r)^2}{r^2} \cdot \frac{1}{2}}_{\leq 0} \iff \gamma'_1 = 0 \vee \frac{(m-r)^2}{r^2} = 0$.

Note that $\gamma'_1 = 0$ implies, on the one hand, that $\gamma' = \gamma'_1 \partial_\nu + \gamma'_2 \partial_r = 0$, which means γ' is not future pointing.

On the other hand, the solution to $\frac{(m-r)^2}{r^2} = 0$ gives $r = m$, which is the horizon and is not part of region M_2 . Hence, we conclude that $\frac{dr}{ds} = \gamma'_2 < 0$, as claimed. \square

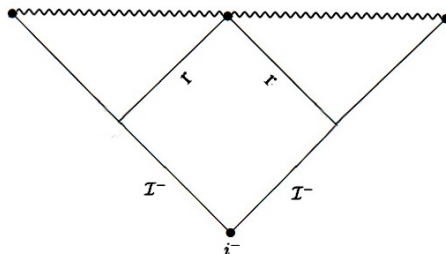


FIGURE 11. Conformal diagram for the extremal pseudo-Reissner-Nordström spacetime.

From these results, and given that r is strictly monotonic decreasing, we can conclude that for a future-pointing timelike curve—as defined above—it is impossible to form a closed curve. Therefore, the extremal pseudo-Reissner-Nordström spacetime does not contain closed timelike curves (CTCs). A closed lightlike curve exists only at $r = m$. Although the extremal pseudo-Reissner-Nordström spacetime does not permit closed timelike curves, a CTC almost emerges at $r = m$. If the light cones were to open up slightly more at that point, chronology would be violated.

6.3. Pseudo-Reissner-Nordström timelike geodesics. We first observe that the geodesics exhibit behavior similar to those in the pseudo-Schwarzschild or Misner space. This becomes evident when we write down the explicit timelike geodesic equation as a function of the radius by substituting $g_{\nu\nu} = -\left(\frac{2m}{r} - \frac{q^2}{r^2} - 1\right)$ into Equation (3.7) in Section 3:

$$(6.4) \quad \nu(r) = \int \frac{\frac{-1}{\left(\frac{2m}{r} - \frac{q^2}{r^2} - 1\right)} \left(\xi - \omega \sqrt{\xi^2 - \left(\frac{2m}{r} - \frac{q^2}{r^2} - 1\right)} \right)}{\omega \sqrt{\xi^2 - \left(\frac{2m}{r} - \frac{q^2}{r^2} - 1\right)}} dr.$$

Such a timelike geodesic with $\xi = 0$ encircles the horizon, while a geodesic with $\xi > 0$ crosses the horizon. For the latter case we consider $\xi^2 = \frac{2m}{r} - \frac{q^2}{r^2} - 1 \iff (\xi^2 + 1)r^2 - (2m)r + q^2 = 0$.

By virtue of the discriminant

$$D = 4m^2 - 4q^2(\xi^2 + 1) \geq 0 \iff m^2 \geq q^2(\xi^2 + 1),$$

we obtain two potential turning points at

$$(6.5) \quad r_{turn1,2} = \frac{2m \pm \sqrt{4(m^2 - q^2(\xi^2 + 1))}}{2(\xi^2 + 1)} = \frac{m \pm \sqrt{m^2 - q^2(\xi^2 + 1)}}{(\xi^2 + 1)}.$$

As our focus in this work is to elaborate on and demonstrate the similarities between the three different spacetimes, we will disregard r_{turn2} and instead direct our attention to the region $M_1 \cup M_2$, specifically to the turning point contained within that region:

$$(6.6) \quad r_{turn1} = \frac{m + \sqrt{m^2 - q^2(\xi^2 + 1)}}{(\xi^2 + 1)}.$$

We observe an analogous situation to the pseudo-Schwarzschild case, where we obtain the corresponding turning point $r_{turn} = \frac{2m}{(\xi^2 + 1)}$ when setting $q = 0$. The behavior of the null geodesics can be derived from the equation

$$\nu(r) = \int \frac{-1}{\left(\frac{2m}{r} - \frac{q^2}{r^2} - 1\right)} (\omega - 1) dr.$$

Analogous to the previously discussed cases, we have a set of null geodesics, specifically $\nu(r) = \text{const}$, that crosses the surfaces at $r = r_{\pm}$. These geodesics are complete and extend from $r = 0$ to $r = \infty$. In contrast, another set of geodesics spirals around the horizons at $r = r_{\pm}$, and as a result, these geodesics are incomplete within this coordinate patch.

Due to the geodesic incompleteness, the embedded pseudo-Reissner-Nordström cylinder with $\theta = \text{const}$ and $\phi = \text{const}$, restricted to $M_1 \cup M_2$, resembles the situation in the 2-dimensional Misner space and cylindrical pseudo-Schwarzschild spacetime.

7. ISOCAUSALITY

In this section we investigate the causal equivalence properties—in the sense of *isocausality* as introduced by García-Parrado and Senovilla—between the three model spacetimes considered in this work: the Misner spacetime (\mathcal{M}_M, g_M) , the pseudo-Schwarzschild spacetime $(\mathcal{M}_{PS}, g_{PS})$, and the pseudo-Reissner-Nordström spacetime $(\mathcal{M}_{PRN}, g_{PRN})$.

Definition 1 (Isocausality). *Two time-oriented spacetimes (\mathcal{M}, g) and (\mathcal{N}, h) are isocausal if there exist smooth maps*

$$\Phi : \mathcal{M} \longrightarrow \mathcal{N}, \quad \Psi : \mathcal{N} \longrightarrow \mathcal{M}$$

such that both Φ and Ψ are causal, i.e. their differentials map future-directed causal vectors to future-directed causal vectors. No bijectivity or inverse relationship between Φ and Ψ is required by this definition.

In several results below we prove a *stronger* property: the causal maps Φ and Ψ are actually mutual diffeomorphisms (smooth bijections with smooth inverses that are also causal) on the universal covers and on certain causally regular regions of the spacetimes. For the compactified models, global mutual diffeomorphisms exist only under an explicit equivariance condition relating the deck group actions; without this condition, isocausality in the strict sense is generally not guaranteed.

Each of our model spacetimes is a warped product

$$\mathcal{M}_i = \mathcal{M}_i^{(Z)} \times_r H^2$$

with 2-dimensional Lorentzian base $(\mathcal{M}_i^{(Z)}, g_i^{(Z)})$ admitting coordinates (ν, r) in which the metric takes the canonical Eddington-Finkelstein-type form

$$(7.1) \quad g_i^{(Z)} = f_i(r) d\nu^2 + 2 d\nu dr,$$

and H^2 the hyperbolic space of constant negative curvature endowed with its standard metric g_{H^2} . The explicit functions $f_i(r)$ for $i = M, PS, PRN$ have been given in the preceding sections.

Because all three bases share the same canonical structure (7.1), one expects the existence of explicit coordinate transformations mapping each $g_i^{(Z)}$ to any other $g_j^{(Z)}$ up to a smooth, strictly positive conformal factor. Such transformations preserve the null cones on the base and, when extended trivially over H^2 , preserve the full causal structure of the warped product. This observation motivates the main results of this section:

- In Proposition 7.1 we construct explicit causal bijections between the universal covers of the three models, proving that they are *pairwise isocausal* in the covering space. We also identify causally regular regions in the original spacetimes on which the same holds.
- Part (C) of Proposition 7.1 provides a clean necessary and sufficient condition (equivariance with respect to the deck group actions and single-valuedness of the conformal factor) under which the isocausality descends to the compactified spacetimes.
- Corollary 1 clarifies that, in the absence of such equivariance, one obtains only a one-way causal relation between the compactified models.
- Remark 7.2 emphasizes that this one-way causal relation should be regarded as the *generic* global situation unless the deck-group matching is verified explicitly.

We now turn to the formal statements and proofs.

Proposition 7.1 (Isocausality of the Misner-type family). *Let (\mathcal{M}_M, g_M) be Misner spacetime, $(\mathcal{M}_{PS}, g_{PS})$ the pseudo-Schwarzschild spacetime, and $(\mathcal{M}_{PRN}, g_{PRN})$ the pseudo-Reissner-Nordström spacetime, with the $1 + 1$ radial (base) metrics written in the canonical Eddington-Finkelstein-type form*

$$(7.2) \quad g^{(Z)} = f(r) dv^2 + 2 dv dr,$$

where, on the base coordinates used in this paper,

$$f_M(T) = T, \quad f_{PS}(r) = -\left(\frac{2m}{r} - 1\right), \quad f_{PRN}(r) = -\left(\frac{2m}{r} - \frac{q^2}{r^2} - 1\right),$$

and the full 4-metrics are the warped products $g_i = g_i^{(Z)} \oplus r^2 g_{H^2}$ with the hyperbolic fiber H^2 . Denote universal covers by $(\widetilde{\mathcal{M}}_i, \widetilde{g}_i)$ and the covering projections by π_i .

(A) Local / covering isocausality. For every pair $(i, j) \in \{M, PS, PRN\}^2$ there exists a smooth bijection

$$\widetilde{\Phi}_{ij} : \widetilde{\mathcal{M}}_i \longrightarrow \widetilde{\mathcal{M}}_j$$

whose differential preserves future-directed causal vectors and whose inverse $\widetilde{\Phi}_{ji} = \widetilde{\Phi}_{ij}^{-1}$ has the same property.

In particular the universal covers $(\widetilde{\mathcal{M}}_i, \widetilde{g}_i)$ are pairwise isocausal in the García-Parrado-Senovilla sense.

(B) Isocausality on causally regular regions. Let $U_i \subset \mathcal{M}_i$ denote open regions obtained by removing (a) neighborhoods of curvature singularities, and (b) neighborhoods of null hypersurfaces where $f_i = 0$, so that f_i is smooth and nowhere zero on U_i and the S^1 -orbits (if present) can be unwrapped. Then for every pair (i, j) there exists a diffeomorphism $\Phi_{ij} : U_i \rightarrow U_j$ such that both Φ_{ij} and Φ_{ij}^{-1} map future-directed causal vectors to future-directed causal vectors; i.e. (U_i, g_i) and (U_j, g_j) are isocausal.

(C) Global isocausality (quotient) criterion. If the covering-space diffeomorphism $\widetilde{\Phi}_{ij}$ constructed in (A) is equivariant with respect to the deck groups (periodic identifications) Γ_i, Γ_j —meaning there exists $k \in \{\pm 1\}$ such that

$$\widetilde{\Phi}_{ij} \circ \gamma = \gamma^k \circ \widetilde{\Phi}_{ij} \quad \text{for all } \gamma \in \Gamma_i,$$

and if the induced conformal factor descends to a smooth, strictly positive single-valued function on the quotient—then $\tilde{\Phi}_{ij}$ descends to a smooth map

$$\Phi_{ij} : \mathcal{M}_i \longrightarrow \mathcal{M}_j$$

that is a global causal bijection with causal inverse. In this case (\mathcal{M}_i, g_i) and (\mathcal{M}_j, g_j) are globally iscausal. If the equivariance condition fails (periods mismatch, or conformal factor not single-valued), the covering-space result does not imply global iscausality; at most a one-way causal relation $\mathcal{M}_i \prec \mathcal{M}_j$ can be guaranteed.

Proof. We prove (A)–(C) by an explicit local construction on the $1+1$ bases and then extend trivially on the hyperbolic fiber.

Step 1: choice of domains. Fix any pair (i, j) and choose open domains on the corresponding bases where f_i and f_j are smooth and nonvanishing (exclude neighborhoods of roots of f and curvature singularities). On these domains the metrics are nondegenerate and causal cones are well defined.

Step 2: tortoise coordinate and model map. For each model define a (local) tortoise coordinate r_i^* by any smooth antiderivative of

$$\frac{dr}{dr_i^*} = \frac{|f_i(r)|}{2},$$

so that $dr_i^* = (2/|f_i|) dr$. (Any smooth choice suffices on the fixed domain.) Fix a nonzero constant $\alpha \in \mathbb{R}$ and define a map on the $1+1$ base by

$$(7.3) \quad (\nu, r) \longmapsto (\phi, R) = \left(\phi = \alpha \nu, R = \exp(\alpha r_i^*(r)) \right).$$

Extend this map trivially on the hyperbolic fiber $(\theta, \varphi) \mapsto (\theta, \varphi)$ to obtain a map $\tilde{\Phi}_{ij}$ between the corresponding covered regions of $\tilde{\mathcal{M}}_i$ and $\tilde{\mathcal{M}}_j$.

Step 3: pullback computation and conformal factor. A direct computation (cf. the calculation in Sec. 5.1.1) gives, on the base,

$$\tilde{\Phi}_{ij}^*(f_j(R) d\phi^2 + 2 d\phi dR) = \Omega_{ij}(r) (f_i(r) d\nu^2 + 2 d\nu dr),$$

where the factor $\Omega_{ij}(r)$ is a smooth function determined by f_i, f_j, α and $r_i^*(r)$. Because $R > 0$ and r_i^* is smooth, one checks that $\Omega_{ij}(r) > 0$ on the chosen domain (in particular one may choose α so that Ω_{ij} is positive everywhere on the domain). Thus the pullback equals the source metric times a strictly positive conformal factor.

Conformal rescalings preserve null cones in $1+1$ dimensions (and more generally they preserve the causal character of vectors), hence $d\tilde{\Phi}_{ij}$ maps future-directed causal vectors of \tilde{g}_i to future-directed causal vectors of \tilde{g}_j . The inverse map is obtained by reversing the change of variables: given (ϕ, R) , recover $r_j^* = \alpha^{-1} \ln R$, then invert $r_j^* \mapsto r$ and set $\nu = \alpha^{-1} \phi$. The same computation applied in the reverse direction produces a smooth positive conformal factor for $\tilde{\Phi}_{ji}$, so the inverse is also causal. This proves (A): the universal covers admit mutual causal bijections and are therefore pairwise iscausal.

Step 4: extension to warped product and causally regular regions. The full 4-metric is the warped product $g_i = g_i^{(Z)} \oplus r^2 g_{H^2}$. Since the fiber metric g_{H^2} is Riemannian (positive definite), the causal sign of a tangent vector $X = (X_Z, X_H)$ is determined by the base component up to the positive contribution of the fiber weighted by r^2 . With $\tilde{\Phi}_{ij}^*(g_j^{(Z)}) = \Omega_{ij} g_i^{(Z)}$ and the fiber left unchanged (or mapped identically), one has

$$\tilde{\Phi}_{ij}^*(g_j)(X, X) = \Omega_{ij} g_i^{(Z)}(X_Z, X_Z) + (r_j \circ \tilde{\Phi}_{ij})^2 g_{H^2}(X_H, X_H).$$

Because $\Omega_{ij} > 0$ and g_{H^2} is positive definite, the causal cone on the pulled-back metric coincides with that of g_i up to the positive scaling; therefore $\tilde{\Phi}_{ij}$ preserves causal directions on the full 4-space. Restricting to

quotient regions $U_i \subset \mathcal{M}_i$ where periodic identifications have been removed (or after passing to universal covers) gives the statement (B).

Step 5: descent / equivariance criterion (C). The maps above are constructed on universal covers. The covering projections $\pi_i : \widetilde{\mathcal{M}}_i \rightarrow \mathcal{M}_i$ have deck groups $\Gamma_i \cong \mathbb{Z}$ generated by the periodic identification in the angular/cylindrical coordinate. If $\widetilde{\Phi}_{ij}$ satisfies the equivariance condition $\widetilde{\Phi}_{ij} \circ \gamma = \gamma^k \circ \widetilde{\Phi}_{ij}$ for all $\gamma \in \Gamma_i$ and some fixed $k = \pm 1$, then $\widetilde{\Phi}_{ij}$ descends to a well defined smooth map $\Phi_{ij} : \mathcal{M}_i \rightarrow \mathcal{M}_j$ with $\pi_j \circ \widetilde{\Phi}_{ij} = \Phi_{ij} \circ \pi_i$. Since $d\widetilde{\Phi}_{ij}$ preserves causal cones and the conformal factor is single-valued and strictly positive on the quotient by equivariance, the descended map $d\Phi_{ij}$ also preserves future-directed causal vectors. The inverse descends as well (equivariance for the inverse follows from equivariance of the original map), so Φ_{ij} is a global causal bijection with causal inverse: the compactified quotients are globally isocausal. If equivariance fails (periods mismatch or the conformal factor is multi-valued on the quotient) then the composition $\pi_j \circ \widetilde{\Phi}_{ij} \circ \pi_i^{-1}$ fails to be a bijection (or fails to be single-valued) and one obtains at best a one-way causal map $\mathcal{M}_i \rightarrow \mathcal{M}_j$ (hence $\mathcal{M}_i \prec \mathcal{M}_j$ but not necessarily the converse).

This completes the proof of (A)–(C). \square

Corollary 1 (Default global outcome without equivariance). *Let (\mathcal{M}_i, g_i) and (\mathcal{M}_j, g_j) be any two of the Misner, pseudo-Schwarzschild, or pseudo-Reissner-Nordström spacetimes. Suppose there exists an isocausality diffeomorphism*

$$\widetilde{\Phi}_{ij} : \widetilde{\mathcal{M}}_i \longrightarrow \widetilde{\mathcal{M}}_j$$

between their universal covers, as in Proposition 7.1(A), but that the equivariance hypothesis in Proposition 7.1(C) fails (e.g. the deck-group periods do not match up to an integer winding, or the conformal factor is not single-valued on the quotient). Then the descended map

$$\Phi_{ij} := \pi_j \circ \widetilde{\Phi}_{ij} \circ \pi_i^{-1} : \mathcal{M}_i \longrightarrow \mathcal{M}_j$$

is a well-defined smooth causal map (future-directed causal vectors are mapped to future-directed causal vectors), but Φ_{ij} need not be bijective nor admit a causal inverse on the quotient. Thus, in the absence of deck-equivariance, one has only the one-way causal relation

$$\mathcal{M}_i \prec \mathcal{M}_j$$

globally, despite mutual isocausality at the covering level.

Proof. Let $\pi_i : \widetilde{\mathcal{M}}_i \rightarrow \mathcal{M}_i$ and $\pi_j : \widetilde{\mathcal{M}}_j \rightarrow \mathcal{M}_j$ be the universal covering projections, and let $\widetilde{\Phi}_{ij} : \widetilde{\mathcal{M}}_i \rightarrow \widetilde{\mathcal{M}}_j$ be the causal diffeomorphism between covers whose existence is asserted in Proposition 7.1(A). Denote by Γ_i and Γ_j the corresponding deck groups. Recall that a map $\widetilde{\Phi}_{ij}$ descends to a well-defined map $\Phi_{ij} : \mathcal{M}_i \rightarrow \mathcal{M}_j$ if and only if it is equivariant with respect to the deck actions, i.e. there exists $k \in \{\pm 1\}$ such that

$$\widetilde{\Phi}_{ij} \circ \gamma = \gamma^k \circ \widetilde{\Phi}_{ij} \quad \text{for all } \gamma \in \Gamma_i.$$

If equivariance fails then there exists $\gamma \in \Gamma_i$ for which $\widetilde{\Phi}_{ij} \circ \gamma \neq \gamma^k \circ \widetilde{\Phi}_{ij}$ for every $k \in \{\pm 1\}$. Pick any $x \in \mathcal{M}_i$ and choose two distinct lifts $\tilde{x}, \tilde{x}' = \gamma \tilde{x} \in \widetilde{\mathcal{M}}_i$. Then

$$\pi_j(\widetilde{\Phi}_{ij}(\tilde{x})) \quad \text{and} \quad \pi_j(\widetilde{\Phi}_{ij}(\tilde{x}'))$$

are the two candidate values for a putative descended map $\Phi_{ij}(x)$ obtained by composing the projections with $\widetilde{\Phi}_{ij}$. But, because equivariance fails, these two points need not coincide in \mathcal{M}_j , so the composition

$$\pi_j \circ \widetilde{\Phi}_{ij} \circ \pi_i^{-1}$$

is not single-valued on \mathcal{M}_i and hence does not define a well-defined map $\Phi_{ij} : \mathcal{M}_i \rightarrow \mathcal{M}_j$.

Consequently, the cover construction alone does not produce a canonical causal map between the compactified spacetimes unless equivariance holds. Since isocausality of (\mathcal{M}_i, g_i) and (\mathcal{M}_j, g_j) requires the existence of causal maps in both directions on the *quotients* themselves, the failure of descent means that global isocausality cannot be concluded from the covering diffeomorphism without an independent argument that either (i) a descended causal map exists by some other construction, or (ii) the equivariance obstruction can be removed. This completes the proof. \square

Remark 7.2 (On the generic global situation). In the absence of an explicit verification of the deck-equivariance condition in Proposition 7.1(C), the generic expectation for the compactified Misner-type spacetimes considered here is that mutual isocausality will *not* hold globally, even though their universal covers are mutually isocausal. Without equivariance, any global causal relationship must be established by direct construction, and may exist in only one direction.

Physical meaning of global vs. covering isocausality. The distinction between isocausality at the level of the universal covers and the compactified spacetimes has a clear operational interpretation. On the universal cover, the causal structure is the “local” one perceived by any observer restricted to a simply connected region: the shape of the light cones, the accessibility of events along causal curves, and the arrangement of horizons are indistinguishable across the three models. In this sense, freely falling observers with access only to local measurements would not be able to tell which spacetime they inhabit; the causal physics is the same.

However, when passing to the compactified spacetimes by quotienting along closed orbits, additional global identifications introduce genuinely new causal phenomena, most notably the appearance and arrangement of closed timelike curves (CTCs). Failure of the deck-equivariance condition means that these identifications differ between the models: a causal curve that is closed in one model may fail to be closed in another, or the chronology-violating set may have a different extent. Operationally, an observer traversing a large loop along a timelike orbit in one spacetime might return to their starting event, while in another spacetime with the same local light cone structure they would not—or would reappear at a different event. Thus, the one-way causal relation $\mathcal{M}_i \prec \mathcal{M}_j$ reflects the fact that every causal path available in \mathcal{M}_i is realisable in \mathcal{M}_j , but not necessarily the other way around. This is a genuinely global effect that cannot be detected from purely local measurements.

8. CONCLUSION

We have investigated a family of causality-violating spacetimes—specifically, the pseudo-Schwarzschild, pseudo-Reissner-Nordström, and Misner spacetimes—that share fundamental causal structures, including the presence of chronology horizons, Cauchy horizons, radial geodesics, and acausal regions. All these spacetimes can be expressed in a warped product form, with metrics decomposing into the cylindrical metric g_Z and the hyperbolic metric g_{H^2} . This structure allows us to focus on their 2-dimensional cylindrical analogues. In Eddington-Finkelstein coordinates, these cylindrical versions can be brought to a canonical form $ds^2 = g_{\nu\nu}d\nu^2 + 2g_{\nu r}d\nu dr$, from which the radial geodesic equations (Section 3) can be systematically derived. Renaming the coordinates as $\nu = \varphi$ and $r = T$, the connection to Misner spacetime becomes manifest.

In each case, the base manifold M_Z of the warped product structure is conformally related to a region of Minkowski spacetime and admits a Killing vector field whose orbits closely resemble those of the boost-generating vector field $X = x\partial_t + t\partial_x$ in two-dimensional Minkowski space. This Killing vector field generates a one-parameter group G of isometries, some of whose orbits are timelike. A discrete subgroup $G_0 \subset G$ acts properly and freely on M_Z , resulting in a Misner-like structure on the quotient M_Z/G_0 , where the timelike

orbits of G project to closed timelike curves.¹¹ From a mathematical standpoint, this conformal structure renders the similarities in causal properties relatively unsurprising, as they directly reflect known features of Misner spacetime. Nevertheless, from a physics perspective, the results are noteworthy. The spacetimes examined differ markedly in their physical interpretation and geometric origin—ranging from a flat vacuum solution of the Einstein equations, to an asymptotically flat black hole solution of the vacuum Einstein equations, to a model that violates the weak energy condition and requires ‘exotic matter’ as its source—yet they exhibit analogous causal behavior. Understanding these similarities across physically distinct settings provides valuable insights into how causality can be broken or preserved under varying geometrical and physical conditions.

A central result of this work is the formal proof of the *isocausality* of the Misner-type family at the covering level. In Proposition 7.1 we showed that the universal covers of the Misner, pseudo-Schwarzschild, and pseudo-Reissner-Nordström spacetimes are *pairwise isocausal* via explicit smooth bijections whose differentials preserve and reflect all future-directed causal cones. This isocausality also holds on suitable open, causally regular regions of the compactified spacetimes where the chronology-violating sets and Cauchy horizons are excised. Furthermore, we identified an explicit and checkable *deck-equivariance criterion* under which the isocausality descends to the full compactified spacetimes. When this criterion fails, Corollary 1 and Remark 7.2 show that the covering-space result does not imply global isocausality, and one should expect only a *one-way causal relation* between the compactified models. This distinction between local/covering and global/quotient behavior is essential for understanding the true strength of the causal equivalences in these examples.

In the context of ongoing research on spacetimes with closed timelike curves [1, 4, 9, 19], our findings offer a unified framework to view several causality-violating spacetimes through a common geometric and causal lens. The work reveals the intricate relationships between these examples and motivates a broader investigation into the interplay between geometry, causality, and spacetime topology. For instance, it would be compelling to investigate whether other spacetime models, such as the pseudo-Kerr spacetime [3]—a rotating generalization of the pseudo-Schwarzschild metric—also belong to this family of causality-violating, Misner-type spacetimes.

We view this article as a step toward a broader classification of causality-violating spacetimes. The warped-product ansatz and the explicit isocausality mappings presented here suggest that tools from conformal geometry and causal theory can provide a systematic framework for organising, comparing, and understanding causal structures in a wide range of gravitational models.

Acknowledgement. Parts of this work were completed during my time as a member of Richard Schoen’s research group at the University of California, Irvine. However, the research presented here originated from a project conducted under the supervision of Kip S. Thorne during 2016-2018. I am profoundly grateful to Kip S. Thorne for his invaluable advice, guidance, supportive remarks, and encouragement throughout the course of this work. I would also like to express my deep appreciation for his inspiring spirit of intellectual adventure in research and the insightful discussions, particularly on Misner space, which have been truly indispensable to this work. Furthermore, I am very grateful to the referees for their thorough and constructive feedback.

¹¹As described in the classic book by Hawking and Ellis [11], Misner space is constructed by taking a quotient of half of Minkowski spacetime under a discrete subgroup of the one-parameter isometry group generated by the vector field $X = x \partial_t + t \partial_x$, which acts properly and freely in that region. A similar isometry group orbit structure appears in the (t, r) -planes of both the Schwarzschild and Reissner–Nordström spacetimes, allowing for analogous quotient constructions in these cases as well.

REFERENCES

- [1] A. Awad and S. Eissa. Lorentzian Taub-NUT spacetimes: Misner string charges and the first law. *Phys. Rev. D*, 105 (2022), 124034.
- [2] S. Chandrasekhar. *The Mathematical Theory of Black Holes*. Clarendon Press, Oxford, England and Oxford University Press, New York (1983).
- [3] J. Dietz, A. Dirmeier and M. Scherfner. Geometric analysis of particular compactly constructed time machine spacetimes. *J. Geom. Phys.*, 62 (2012), 1273–1283.
- [4] R. Emparan and M. Tomašević. Quantum backreaction on chronology horizons. *J. High Energ. Phys.*, 2022, 182 (2022).
- [5] V. Frolov and I. Novikov. *Black Hole Physics: Basic Concepts and New Developments*. Springer Dordrecht (1998).
- [6] A. García-Parrado and J. M. M. Senovilla. Causal relationship: A new tool for the causal characterization of Lorentzian manifolds. *Class. Quantum Grav.* 20 (2003), 625–664.
- [7] A. García-Parrado and M. Sánchez. Further properties of causal relationship: Causal structure stability, new criteria for isocausality and counterexamples. *Class. Quantum Grav.* 22 (2005), 4589–4619.
- [8] M. Gaudin, V. Gorini, A. Kamenshchik, U. Moschella and V. Pasquier. Gravity of a static massless scalar field and a limiting Schwarzschild-like geometry. *Int. J. Mod. Phys. D* 15 (2006).
- [9] L. Gavassino. Life on a closed timelike curve. *Class. Quantum Grav.* 42 (2025), 015002.
- [10] R. Göhring. *Kosmologie der allgemeinen Relativitätstheorie*. Physikalischer Verein, Frankfurt am Main (2010).
- [11] S. W. Hawking and G. F. R. Ellis. *The Large Scale Structure of Space-Time*. Cambridge University Press, Cambridge (1973).
- [12] S. Kim and K. S. Thorne. Do vacuum fluctuations prevent the creation of closed timelike curves? *Phys. Rev. D*, 43 (1991), 3929.
- [13] D. A. Konkowski and L. C. Shepley. Stability of Two-Dimensional Quasisingular Space-Times. *Gen. Relativ. Gravit.* 14, No. 1 (1982).
- [14] C. W. Misner. Taub-NUT Space as a Counterexample to Almost Anything. *Relativity Theory and Astrophysics I: Relativity and Cosmology* (J. Ehlers Ed.), Lectures in Applied Mathematics 8 A.M.S. (1967).
- [15] C. W. Misner, K. S. Thorne and J. A. Wheeler. *Gravitation*. W. H. Freeman and Company, NY, San Francisco (1973).
- [16] A. Ori. Formation of closed timelike curves in a composite vacuum-dust asymptotically flat spacetime. *Phys. Rev. D*, 76 (2007), 044002.
- [17] D. Levanony and A. Ori. Extended time-travelling objects in Misner space. *Phys. Rev. D*, 83 (2011), 044043.
- [18] N. E. Rieger. Topologies of maximally extended non-Hausdorff Misner Space. arXiv:gr-gc/2402.09312 (2024), digital preprint of the 2016 original version.
- [19] D. Roy, A. Dutta and S. Chakraborty. Geodesic Motion and Particle Confinements in Cylindrical Wormhole Spacetime: Exploring Closed Timelike Curves. *Int. J. Mod. Phys. A* (2025).
- [20] P. Sharan. *Spacetime, Geometry and Gravitation*. Springer, Birkhäuser Basel (2009).
- [21] K. S. Thorne. Closed Timelike Curves. *General Relativity and Gravitation; Proceedings of the 13th International Conference on General Relativity and Gravitation*, Institute of Physics Publishing, Bristol, England (1993), 295–315.
- [22] K. S. Thorne. Misner Space as a Prototype for Almost Any Pathology. *Directions in General Relativity* Eds. B. L. Hu et al., Cambridge University Press, Cambridge (1993), 333–346.